Earth-Science Reviews xxx (xxxx) xxx-xxx

Contents lists available at ScienceDirect

Earth-Science Reviews

journal homepage: www.elsevier.com

Textural signatures of sediment supply in gravel-bed rivers: Revisiting the armour ratio

Daniel Vázquez-Tarrío [a,*], Hervé Piégay [a], Rosana Menéndez-Duarte [b,c]

[a] University of Lyon, CNRS UMR 5600 EVS, Site ENS, F-69342 Lyon, France
[b] Department of Geology, University of Oviedo, c\ Jesús Arias de Velasco, s/n, 33005 Oviedo, Spain
[c] INDUROT, University of Oviedo, Campus de Mieres, s/n, 33600 Mieres, Spain

ARTICLE INFO

Keywords:
Gravel-bed rivers
Armour ratio
Sediment supply
Bedload

ABSTRACT

The surface of the streambed in gravel-bed rivers is commonly coarser than the underlying bed material. This surface coarsening, or 'armouring', is usually described by means of the ratio between surface and subsurface grain-size metrics (the 'armour ratio'). Such surface coarsening is typical of river reaches that are degrading due to a deficit in sediment supply (e.g. gravel-bed reaches below dams or lakes), but non-degrading gravel-bed streams may also exhibit some degree of armouring in relation to specific hydrological patterns. For instance, selective transport during the recession limbs of long lasting floods may coarsen the bed more significantly than flash floods. Consequently, regional differences in bed coarsening should exist, reflecting in turn the variability in sediment and water regimes. In this paper, we explore the trends linking armour ratios to sediment supply, taking into account the differences in hydrological context. We based our analysis on a large data set of bedload and grain size measurements from 49 natural gravel-bed streams and four flume experiments compiled from the scientific literature. Our main outcome documents how the balances between sediment yields and transport capacities have a quantifiable reflection on the armour ratios measured in the field: we report statistically significant correlations between bedload fluxes and surface grain-size, and an asymptotic rise in armour ratios with the decline of sediment supply. Hydrological controls are also observed. Additionally, the trends observed in the field data are comparable to those previously documented in flume experiments with varying sediment feed. In this regard, different kinds of bedforms and particle arrangements have been commonly described with progressive reductions in sediment inputs and the subsequent coarsening of the streambed. Hence, armour ratios serve as a proxy for the general organization of the streambed of gravel-bed streams, and our results quantify this streambed adjustment to the dominant sediment regime.

1. Introduction

A longstanding idea in fluvial geomorphology is that balances between sediment supply and transport capacities influence channel geometry (Parker et al., 2007; Parker, 2008), bed slope (e.g. Lane, 1955a; Borland, 1960; Wilcock et al., 2009), streambed texture (Dietrich et al., 1989; Nelson et al., 2009; Venditti et al., 2017) and planform morphology (e.g. Montgomery and Buffington, 1997; Church, 2006; Buffington, 2012; Hassan and Zimmermann, 2012; Métivier and Barrier, 2012). Thus, an abiding goal for a great deal of research in river morphodynamics has searched for a quantitative comprehension of channel adjustments to the balance between water and sediment supply (e.g. Lane, 1955a, 1955b; Parker, 2004; Blom et al., 2017), yet a full understanding still needs to be elucidated (Eaton et al., 2004; Lawson, 2020). In particular, the prediction of how riverbed texture responds to changes in governing conditions (discharge, sediment supply, valley slope) remains elusive. Very often, the evolution of bed texture is neglected from morphodynamic models or treated with simplistic approaches (Lawson, 2020), even though bed state is a main regulator of river response to sediment supply fluctuations (e.g. Church et al., 1998; Clayton and Pitlick, 2008; Turowski et al., 2011).

In this regard, one major sedimentary feature in gravel-bed rivers is streambed coarsening (often called 'armouring'). Early field observations (e.g. Harrison, 1950; Gessler, 1967; Willets et al., 1988; Richards and Clifford, 1991) realized that surface coarsening was a pervasive textural feature of gravel-bed rivers. Since then, armouring has been typically reported in degrading beds and river reaches with low or no sediment supply (e.g. gravel-bed reaches downstream from dams or lakes) (Gessler, 1967; Willets et al., 1988; Jain, 1990; Chin et al., 1994; Gomez, 1994; Vericat et al., 2006). In such cases, surface armours

* Corresponding author.
Email address: daniel.vazquez_tarrio@ens.fr (D. Vázquez-Tarrío)

https://doi.org/10.1016/j.earscirev.2020.103211
Received 5 November 2019; Received in revised form 4 May 2020; Accepted 17 May 2020
Available online xxx
0012-8252/ © 2020.

were called ‘static’ or ‘pavement’ (Jain, 1990; Yager et al., 2015; Bertin and Friedrich, 2018) and their development is likely driven by sediment winnowing during low flood flows (Gomez, 1983, 1993, 1994). Static armours can ‘breakup’ during high flow peaks and/or transport episodes with large sand sediment supplies (Laronne and Carson, 1976; Gomez, 1983; Klaassen, 1988; Vericat et al., 2006) and re-form during the falling limb of the flood hydrograph. Non-degrading gravel-bed streams with considerable sediment inputs also exhibit some armouring due to a combination of winnowing during low discharges and kinematic sorting (Parker and Klingeman, 1982; Wilcock, 2001). In truth, bedload transport models (Wilcock and DeTemple, 2005), tracer studies (Haschenburger and Wilcock, 2003), flume experiments (Hassan et al., 2006), and field observations (Andrews and Erman, 1986; Clayton and Pitlick, 2008; Haschenburger, 2017) support the occurrence of such ‘mobile’ or ‘dynamic’ armours and their persistence even during large floods. Apart from armouring, a large diversity of particle arrangements has been reported in the field for gravel-bed rivers (Cin, 1968; Church et al., 1998; Hassan and Church, 2000; Wittenberg et al., 2007; Hassan et al., 2008), which seem to be more prevalent when sediment supply is low and beds are well armoured.

In addition to field studies, flume experiments also contribute to increase knowledge of how streambed texture responds to the balance between water discharge and sediment supply. In this regard, seminal research by Dietrich et al. (1989) reported how reductions in sediment supply tend to promote active channel narrowing, surface coarsening, bedload fining, and transport rate decrease in gravel-bed rivers. Substantial subsequent work documented the influence of sediment inputs on the spatial and vertical patterns of grain size sorting (Nelson et al., 2009, 2010) and how surface grain-size responds to a decrease in bedload through the expansion of coarse fixed patches (Nelson et al., 2009; Yager et al., 2015), resulting in a general coarsening of the streambed. Flume experiments also tried to elucidate the mechanisms beyond armour development at the grain-scale, such as fine-sediment winnowing during low discharges (Chin et al., 1994; Gomez, 1994), infiltration of fine sediment (Marion and Fraccarollo, 1997; Curran and Waters, 2014; Berni et al., 2018), and kinematic sorting during bed load transport (Wilcock, 2001; Bacchi et al., 2014; Ferdowsi et al., 2017) and on the conditions beyond armour breakup under no sediment supply (Wang and Liu, 2009) or triggered by large fine-sediment inputs (Venditti et al., 2005; Venditti et al., 2010a, 2010b). More recently, Orrú et al. (2016) studied the breakup and reformation of static armours, documenting armour breakup with release of subarmour fines and quick armour reformation during high flows. Hassan et al. (2006) and Plumb et al. (2019) delved into the effects of hydrograph characteristics on surface coarsening, documenting how experiments with flat and sustained hydrographs developed a well-armoured structured surface, while sharply peaked hydrographs did not result in substantial armouring. Follow-up research by Berni et al. (2018) and Hassan et al. (2020) continued exploring the timing of armour formation. In addition, another major line of experimental research investigated the coevolution between armouring and bed structures (e.g., Venditti et al., 2017; Bertin and Friedrich, 2018; Hassan et al., 2020), highlighting the influence of bed structures on bed topography, particle entrainment, and bedload transport (Hassan and Reid, 1990; Gomez, 1993, 1994; Nikora et al., 1998; Butler et al., 2001; Church and Hassan, 2002; Marion et al., 2003; Smart et al., 2004; Cooper and Tait, 2009; Hodge et al., 2009; Mao et al., 2011; Heays et al., 2014; Perret et al., 2020).

In summary, both field and flume research point at the linkages between streambed texture and sediment supply regime as a key question in river morphodynamics and fluvial geomorphology. As we have outlined above, flume research has significantly augmented the theoretical and quantitative understanding of streambed adjustments to sediment supply. Field research, however, has often been case-study focused and the intrinsic complexity of bedload measurement complicates the field assessment of streambed response to sediment supply fluctuations (Pitlick et al., 2012). For these reasons, the question of how well the results from laboratory studies could be extrapolated to interpret field observations is still open. Hence, in the first part of this paper we propose an extensive review of previous flume and field research on gravel-bed rivers, first introducing compiled data from the scientific literature for 49 natural gravel-bed rivers and then addressing surface coarsening and its different controls. We illustrate this literature review by a systematic re-examination of compiled grain-size measurements and bedload discharge. In the second part of the paper, we performed a meta-analysis of the compiled data in order to quantify the covariation of surface coarsening with channel hydraulics, hydrology, and bedload fluxes in natural rivers. The main outcomes of this meta-analysis are twofold: (i) documenting an asymptotic rise in armouring with sediment supply decline; and (ii) reporting some correlation between bedload fluxes, surface grain-size, and channel morphology.

2. Compiled field data

The dataset used in the present paper consists of grain-size and bedload measurements collected at 49 river sites (summarized in Table 1). An important amount of the compiled data derives from the extensive campaign of sediment transport measurements carried out on Idaho, Nevada (King et al., 2004), Colorado, and Wyoming rivers (Ryan et al., 2002, 2005). These data have been presented previously and analysed in several papers (Ryan et al., 2002, 2005; King et al., 2004; Barry et al., 2004; Mueller et al., 2005; Muskatirovic, 2008; Pitlick et al., 2008). The remaining data come from comparable measurements in other gravel-bed streams (Milhous, 1973; Emmett and Seitz, 1974; Seitz, 1977; Jones and Seitz, 1980; Reid and Frostick, 1986; Lisle, 1986, 1989; Williams and Rosgen, 1989; Gomez, 1988; Kuhnle, 1992; Lisle and Madej, 1992; Andrews, 1994; Reid et al., 1995; Madej and Ozaki, 1996; McLean et al., 1999; Almedeij, 2002; Church and Hassan, 2002; Wilcock and Kenworthy, 2002; Church and Rice, 2009; Erwin et al., 2011; Mueller and Pitlick, 2014).

Grain sizes for each selected river were obtained from the tables and/or graphical reading of grain-size curves extracted from the corresponding papers. When bed material was sampled at several times or locations in the same river, we averaged the results to obtain a characteristic grain-size measure for each case study, which may eventually introduce a ~30% variability around the average values for the coarser percentiles of the grain-size distribution (GSD). Stream discharge information is available for the selected case studies, together with width-averaged data on the main flow characteristics (velocity, active width). Using this information, we computed bed shear stress based on Rickenmann and Recking’s (2011) fit to Ferguson’s (2007) friction law. We also compiled, for each case study, values for the representative channel-forming or dominant discharge (Table 2), which were derived from the information provided in the original papers about the bankfull discharge (in single-thread channels) or the ~1 to 2-year return period discharge (in multi-thread channels) (Table 2). Information on bedload discharges and bedload rating curves was also available (Table 1); in this regard, we acknowledge the great work of data compilation carried out by Recking (2010, 2013a), who provided bedload information for these field sites as supporting files.

We grouped the data following three different criteria. We made an initial classification according to dominant channel morphology, grouping the different case studies as riffle and pool, step-pool and plane-bed channels (after Montgomery and Buffington, 1997). Due to its geomorphological significance, we also defined a separate group for multi-thread rivers, in spite of the fact that each single thread of a braided river commonly shows a riffle and pool or bar-pool morphology. We also classified the different data according to the potential sediment supply conditions at the catchment scale (Table 3). Following

Table 1
Sources of field data and information compiled for this study. D_{84}: 84-th percentile of the grain-size distribution (GSD). *Q*: Flow discharges. *Qb*: Bedload discharges. *HS*: Helley-Smith sampler. *N*: number of data. -: Data not available. (?): Inferred from the text.

River/Reach	Source	Channel style	Slope	Surface D_{84} (mm)	Subsurface D_{84} (mm)	GSD measuring method		Flow width (m)	Flow depth (m)	Q (m^3/s)	Qb (g/s·m)	N	Bedload transport sampling method
						Surface	*Subsurface*						
Big Wood River (Idaho, USA)	King et al. *(2004)*	Plane-bed	0.091	250	101	Pebble count and core sampling	Core sampling	12.8	0.4-1.1	6.0-30.9	0.0-336.4	100	HS 7.62 or 15.2 cm (0.25 mm mesh)
Blackmare Creek (Idaho, USA)	King et al. *(2004)*	Plane-bed	0.03	220	97	Pebble count and core sampling	Core sampling	4.94-11.89	0.1-0.5	0.3-4.7	0.0-6.8	88	HS 7.62 or 15.2 cm (0.25 mm mesh)
Boise river (Idaho, USA)	King et al. *(2004)*	Riffle and pool	0.0038	141	86	Pebble count	Core sampling	52.4-61.0	0.6-2.1	33.7-291.7	0.4-633.5	82	HS 7.62 or 15.2 cm (0.25 mm mesh)
Borgne d'Arolla (Switzerland)	Gomez *(1988)*	Step-Pool	0.03	19	12	Contact sampling technique	10 kg-volumetric sampling	0.3-2.2	0.0-0.1	0.0-0.3	56.2-837.0	31	HS (7.6 cm), 0.5 mm mesh
Clearwater River (Idaho, USA)	Jones and Seitz *(1980)*	Riffle and pool	0.00037	70	70	Pebble count	Sieve analysis of dug material	125.0-149.0	3.4-46.3	288.0-3511.0	0.1-284.0	78	HS (7.6 and 15 cm
Dollar Creek (Idaho, USA)	King et al. *(2004)*	Plane-bed	0.0146	145	83	Pebble count and core sampling	Core sampling	7.0-11.9	0.2-0.5	0.4-6.4	0.0-9.7	85	HS 7.62 or 15.2 cm (0.25 mm mesh)
East Fork San Juan (Colorado, USA)	Ryan et al. *(2005)*	Braided	0.008	112	52	Pebble count	Barrel method	15.0-17.2	0.3-0.5	2.8-13.8		77	Wadable version of Elwha sampler, 102 × 203 mm
East Saint-Louis Creek (Colorado, USA)	Ryan et al. *(2002)*	Step-Pool	0.058	142	23	Pebble count	Barrel method	2.8-3.0	0.1-0.4	0.1-1.24	0.0-21.2	109	HS (7.6 cm)
Fool Creek (Colorado, USA)	Ryan et al. *(2002)*	Plane-bed	0.053	100	59	Pebble count	Barrel method	1.7-2.1	0.1-0.2	0.0-0.5	0.0-14.7	95	HS (7.6 cm)
Fraser River (BC, Canada)	McLean et al. *(1999)*; Ferguson and Church *(2009)*	Riffle and pool	0.00046	70	68	Pebble count	Bulk volume sampling	510	-	1085-11445	0.3-486.3	76	Basket sampler (610 × 255 mm) for high flows and half-size VuV sampler (225 × 115 mm) for lower flows
Goodwin Creek (Mississippi, USA)	Kuhnle *(1992)*; Almedeij *(2002)*	Riffle and pool	0.0021	30	30	Pebble count	Bulk volume sampling	11.1-14.6	0.4-1.2	1.4-21.6	0.2-2980.0	357	HS (58 cm2 with trapezoidal shape), 0.25mm net mesh
Harris Creek (BC, Canada)	Church and Hassan *(2002)*	Riffle and pool	0.013	100	55	Pebble count (grid-by-number)	Bulk mass sampling	15	-	4.2-18.4	0.0-4.3	22	Sediment trap
Jacoby (California, USA)	Lisle *(1986)*; Lisle *(1989)*; *Almadeij (2002)*; Wilcock and Kenworthy *(2002)*	Riffle and pool	0.0063	95	81	Pebble count	Frozen core method	17.2	-	0.6-18.51	0.0-413.0	100	HS (4.4 cm)
Johns Creek (Idaho, USA)	King et al. *(2004)*	Step-Pool	0.0207	558	63	Pebble count	Core sampling	8.2-14.6	0.3-1.2	1.0-34.3	0.0-10.7	46	HS 7.62 or 15.2 cm (0.25 mm mesh)
Little Buckhorn Creek (Idaho, USA)	King et al. *(2004)*	Step-Pool	0.0509	340	94	Pebble count and core sampling	Core sampling	1.4-4.6	0.1-0.7	0.1-0.7	0.0-18.5	78	HS 7.62 or 15.2 cm (0.25 mm mesh)
Little Granite Creek (Wyoming, USA)	Ryan et al. *(2002)*	Plane-bed	0.019	220	41	Pebble count	Barrel method	6.5-11.2	-	0.7-11.6	0.0-128.0	123	HS (7.6 cm)
Little Slate (Idaho, USA)	King et al. *(2004)*	Plane-bed	0.0268	380	141	Pebble count and core sampling	Core sampling	6.7-13.4	0.3-1.0	0.5-18.3	0.0-10.3	157	HS 7.62 or 15.2 cm (0.25 mm mesh)
Lochsa river (Idaho, USA)	King et al. *(2004)*	Plane-bed	0.0023	245	123	Pebble count and core sampling	Core sampling	67.1-83.0	1.8-3.1	110.7-758.9	0.0-48.3	72	HS 7.62 or 15.2 cm (0.25 mm mesh))
Lolo Creek (Idaho, USA)	King et al. *(2004)*	Plane-bed	0.0097	140	68	Pebble count and core sampling	Core sampling	10.7-16.0	0.3-1.5	1.8-23.0	0.0-13.4	89	HS 7.62 or 15.2 cm (0.25 mm mesh)
Main Fork Red River (Idaho, USA)	King et al. *(2004)*	Plane-bed	0.0059	93	64	Pebble count and core sampling	Core sampling	6.7-12.3	0.2-1.9	0.3-18.3	0.0-27.7	198	HS 7.62 or 15.2 cm (0.25 mm mesh)
Middle Fork	King et al. *(2004)*	Plane-	0.0041	288	140	Pebble count and core	Core	42.7-67.1	1.2-2.01	83.5-433.2	0.1-727.7	64	HS 7.62 or 15.2 cm (0.25

Table 1 (*Continued*)

River/Reach	Source	Channel style	Slope	Surface D_{84} (mm)	Subsurface D_{84} (mm)	GSD measuring method		Flow width (m)	Flow depth (m)	Q (m^3/s)	Qb (g/s·m)	N	Bedload transport sampling method
						Surface	*Subsurface*						
MF Piedra (Colorado, USA)	Ryan et al. *(2002)*	Riffle and pool	0.011	210	43	Pebble count and core sampling	Core sampling	11.4-13.8	0.2-0.5	1-11.0	0.0-216.6	86	HS 7.62 or 15.2 cm (0.25 mm)
Nahal Yatir (Israel)	Reid et al. *(1995)*	Riffle and pool	0.0088	13	34	Removing clasts from spray-painted stripes and laboratory sieving	Bulk volume sampling	3.5	0.1-0.6	0.3-0.5	200.0-7050.0	74	Sediment trap
North Fork Clearwater (Idaho, USA)	King et al. *(2004)*	Plane-bed	0.0005	270	104	Pebble count and core sampling	Core sampling	9.1-93.6	1.7-34.1	100.8-974.1	0.0-732.2	72	HS 7.62 or 15.2 cm (0.25 mm mesh)
Oak Creek (Oregon, USA)	Milhous *(1973)*	Plane-bed	0.0083	80	52	Pebble count and bottom samplers	Bulk volume sampling	3.7	-	0.0-3.4	0.0-111.0	119	Sediment trap, vortex tube
Pacific creek (Wyoming, USA)	Erwin et al. *(2011)*	Braided	0.0035	45	28	Pebble count	Bulk volume sampling	-	-	-	-	-	-
Rapid River (Idaho, USA)	King et al. *(2004)*	Plane-bed	0.0108	170	101	Pebble count	Core sampling	11.4-18.6	0.2-0.9	0.9-36.8	0.0-294.3	190	HS 7.62 or 15.2 cm (0.25 mm mesh)
Redwood Creek (California, USA)	Lisle and Madej *(1992);* Madej and Ozaki *(1996)*	Riffle and pool	0.0014	18	20	Pebble count	Bulk volume sampling	11.7-70	-	1.8-569	8.1-5067.8	221	HS sampler (7.6 cm)
Saint-Louis Creek (Colorado, USA)	Ryan et al. *(2002, 2005)*	Plane-bed	0.0110-0.0450	162-543	33-78	Pebble count	Barrel method	5.2-10.3	0.1-0.4	0.4-7.2	0.0-65.7	813	HS (7.6 cm)
Sagehen Creek (California, USA)	Andrews *(1994)*	Riffle and pool	0.0102	104	96	Pebble count	Bulk volume sampling	2.6	0.3-1.6	1.0-3.1	0.5-34.9	55	HS (15 cm)
Salmon River below Yankee (Idaho, USA)	King et al. *(2004)*	Plane-bed	0.0034	276	99	Pebble count and core sampling	Core sampling	30.5-38.4	1.2-1.9	38.5-143.6	0.0-98.8	60	HS 7.62 or 15.2 cm (0.25 mm mesh)
Salmon River near Obsidian (Idaho, USA)	King et al. *(2004)*	Plane-bed	0.0066	128	84	Pebble count and core sampling	Core sampling	12.0-14.3	0.7-0.9	7.5-21.0	0.7-103.4	50	HS 7.62 or 15.2 cm (0.25 mm mesh)
Salmon River near Shoup (Idaho, USA)	King et al. *(2004)*	Plane-bed	0.0019	174	136	Pebble count and core sampling	Core sampling	46.5-99.5	1.7-2.7	108.4-540.8	1.0-536.1	60	HS 7.62 or 15.2 cm (0.25 mm mesh)
Selway River (Idaho, USA)	King et al. *(2004)*	Plane-bed	0.0021	265	173	Pebble count and core sampling	Core sampling	82.3-97.8	1.4-2.8	134.8-1067.5	0.0-43.5	72	HS 7.62 or 15.2 cm (0.25 mm mesh)
Silver Creek (Colorado, USA)	Ryan et al. *(2005)*	Plane-bed	0.0450	73	33	Pebble count	Barrel method	3.8-4.4	0.1-0.3	0.1-1.4	0.0-214.3	57	Wadable version of the Elwha sampler, 102 × 203 mm
Snake River (Washington, USA)	Emmett and Seitz *(1974);*Seitz *(1977)*	Riffle and pool	0.0009	115	54	Pebble count	Sieve analysis of dug material	155.4-204.2	3.3-6.2	779.0-4559.0	0.0-342.0	63	HS (7.6 and 15 cm)
Snake River below Jackson Lake (Wyoming, USA)	Mueller and Pitlick *(2014)*	Braided	0.0025	83	58	Pebble count	Bulk volume sampling	-	-	-	-	-	-
South Fork Payette (Idaho, USA)	King et al. *(2004)*	Plane-bed	0.004	150	79	Pebble count and core sampling	Core sampling	43.6-51.8	0.4-1.7	20.4-180.9	-	-	HS 7.62 or 15.2 cm (0.25 mm mesh)
South Fork Red River (Idaho, USA)	King et al. *(2004)*	Plane-bed	0.0146	150	161	Pebble count and core sampling	Core sampling	5.8-12.2	0.1-0.9	0.2-13.0	0.0-29.0	204	HS 7.62 or 15.2 cm (0.25 mm mesh)

Table 1 (*Continued*)

River/Reach	Source	Channel style	Slope	Surface D_{84} (mm)	Subsurface D_{84} (mm)	GSD measuring method		Flow width (m)	Flow depth (m)	Q (m^3/s)	Qb (g/s·m)	N	Bedload transport sampling method
						Surface	*Subsurface*						
Susitna River near Talkeetns (Alaska, USA)	Williams and Rosgen *(1989)*	Braided	0.0015	96	260	Pebble count, bulk sampling (?)	Bulk sampling (?), dredge sampling	118.0-202.0	1.1-14.0	240.0-1310.0	0.9-156.0	39	HS (7.62 cm)
Susitna River at Sunshine, Alaska (Alaska, USA)	Williams and Rosgen *(1989)*	Braided	0.0017	88	163	Pebble count, bulk sampling (?)	Bulk sampling (?), dredge sampling	174.0-311.0	2.1-4.4	504.0-2800.0	33.7-1500.0	41	HS (7.62 cm)
Talkeetna River near Talkeetna (Alaska, USA)	Williams and Rosgen *(1989)*	Braided	0.00096	100	184	Bulk sampling (?)	Bulk sampling (?) dredge sampling	-	-	-	-	-	-
Thompson Creek (Idaho, USA)	King et al. *(2004)*	Plane-bed	0.0153	110	132	Pebble count and core sampling	Core sampling	4.2-6.7	0.2-0.4	0.2-3.5	0.0-38.0	84	HS 7.62 or 15.2 cm (0.25 mm mesh)
Trapper Creek (Idaho, USA)	King et al. *(2004)*	Step-Pool	0.0414	122	67	Pebble count and core sampling	Core sampling	3.5-6.4	0.1-0.6	0.1-3.8	0.0-31.3	166	HS 7.62 or 15.2 cm (0.25 mm mesh)
Turkey Brook (UK)	Reid and Frostick *(1986)*	Riffle and pool	0.0142	42	35	No information	No information	3	0.1-0.9	0.1-13.8	0.0-50.6	206	Pit traps
Valley Creek (Idaho, USA)	King et al. *(2004)*	Plane-bed	0.0040	160	78	Pebble count and core sampling	Core sampling	17.7-42.3	0.4-1.3	3.9-40.2	0.0-56.8	192	HS 7.62 or 15.2 cm (0.25 mm mesh)

Table 2
Information on the dominant channel-forming discharge for the case study selected for the present meta-analysis. ( ) Dominant discharge provided by original authors (*) Bankfull discharge. (**) Dominant discharge provided by Mueller and Pitlick (2014). (***) Reference discharge provided by Church and Rood (1983)

River/Reach	Dominant discharge (m^3/s)	Flow recurrence (years)	River/Reach	Dominant discharge (m^3/s)	Flow recurrence (years)	River/Reach	Dominant discharge (m^3/s)	Flow recurrence (years)	River/Reach	Dominant discharge (m^3/s)	Flow recurrence (years)
Big Wood River	21.7	1.5	Jacoby	19.6	No info	Oak Creek	3.4***	No info	Snake River below Jackson Lake	285**	1.5 - 2
Blackmare Creek	4.7*	1.1	Johns creek	49.0*	3.4	Rapid river	17.7*	1.4	South Fork Payette	86.4*	1.2
Boise river	167.1*	1.7	Little Buckhorn Creek	0.2	1	Pacific creek	60.1	1.5 - 2	South Fork Red River	7.3*	1.5
Borgne d'Arolla	0.2*	< 1	Little Granite Creek	5.9*	1.5	Redwood Creek	560*	2 – 5	Squaw Creek USGS	5.1*	1.6
Clearwater River	2662***	2.2 - 2.3	Little Slate	12.2*	1.4	Saint-Louis Creek	2.6 – 4.8*	1.5	Sunlight Creek-4	16.5**	1.5 - 2
Dollar Creek	6.4*	1.1	Lochsa Creek	446*	1.5	Sagehen Creek	2	~ 1	Sunlight Creek-11	14**	1.5 - 2
East Fork San Juan	15.7*	1.5	Lolo Creek	11.8*	1.2	Salmon River below Yankee	118.1	1.5	Susitna River near Talkeetns	1270**	2
East Saint-Louis Creek	0.9*	1.5	Main Fork Red River	9.3	1.1	Salmon River near Obsidian	12.5	1.5	Susitna River at Sunshine, Alaska	4020**	2
Fool Creek	0.3*	1.5	Middle Fork	217	1.5	Salmon River near Shoup	320	1.5	Talkeetna River near Talkeetna	730**	2
Fraser River	8760	1	Middle Fork Piedra River	10.1*	1.5	Selway River	651.3*	1.7	Thompson Creek	2.5*	1.6
Goodwin creek	10.6	No info	Nahal Yatir	7.9	No info	Silver Creek	1.3*	1.5	Trapper Creek	2.6*	1.9
Harris creek	19.0	1	North Fork Clearwater	453.1*	1.5	Snake River	3426***	2.2 – 2.3	Turkey Brook	19.6	No info
									Valley Creek	24.1*	1.6

Recking et al. (2012), we defined three main groups of data: i. rivers assumed to have low sediment supply, i.e. rivers with channels draining highly vegetated watersheds and no clear active sediment sources and/or alluvial material; ii. rivers with, *a priori*, moderate sediment supply, i.e. rivers located in catchments in which significant bare land areas and/or sparse vegetation, and punctually distributed active sediment sources, are observed; and iii. rivers susceptible to show high sediment supplies, i.e. rivers with channels well-coupled to landslides/slope deposits or fed by strong bank erosion and/or bar-edge trimming (e.g. channels with braided morphology). We based this classification on the scarce information (study site description, photographs, etc.) provided by the original studies and our own inspection of the rivers through Google Earth (Google LLC, various imagery dates: January 2005-January 2019). Nevertheless, available information on measured bedload transport rates at the dominant discharge supports our classification: streams that were classified as having high sediment supplies are those showing larger bedload fluxes and vice versa (Fig. 1). Finally, we also grouped the compiled data according to dominant flow regime, differentiating between i. 'rainfall-dominated'; ii. 'snowmelt/rain-on-snow-dominated'; iii. 'snowmelt-dominated'; iv. 'glacial-fed' and v. 'flash-flood dominated' streams (Table 3). This classification was based on the information provided by the original papers about the hydrological regime.

3. Systematic review of field data on surface coarsening in gravel-bed rivers

3.1. *Surface coarsening in gravel-bed rivers: introducing the 'armour ratio'*

According to both field (e.g. Harrison, 1950; Gessler, 1967; Gomez, 1983; Willets et al., 1988; Richards and Clifford, 1991; Bunte and Abt, 2001) and experimental observations (e.g. Parker and Klingeman, 1982; Dietrich et al., 1989; Parker and Sutherland, 1990; Chin et al., 1994; Parker and Toro-Escobar, 2002) surface coarsening is a widespread textural feature in gravel-bed rivers. Indeed, it has been postulated that surface coarsening represents an intrinsic consequence of bedload transport in poorly sorted gravel-beds, resulting from the adjustment of the streambed's surface to the grain-size distribution of the bedload (Parker and Klingeman, 1982). The compiled field dataset agrees with the conspicuous nature of surface coarsening in gravel-bed rivers, i.e. streambed surface is, in general, coarser than the underlying subsurface GSD (Fig. 2A and 2B). In addition, the percentages of fine sediment are, on average, larger in the subsurface (~15%) than on the surface GSD (~6%) (Fig. 2C). Fine sediment is usually considered to be < 2mm, although some authors define as less than 63 microns to < 4mm. In this paper we consider fine sediment to be < 2 mm, unless otherwise stated. Differences in D_{50} and D_{84} between the surface and the subsurface GSDs persist after truncating the GSDs at 4 mm, so coarsening is not merely related to a major presence of fines in the subarmour bed material (Fig. 2A and 2B). Furthermore, subsurface GSDs are in general more poorly sorted: D_{84}/D_{50} sorting indexes are larger in the subsurface (~3.6 on average) than on the surface GSD (~2.1 on average) (Fig. 2D).

Table 3
Information on sediment-supply at the catchment scale and dominant flow regime for the data compiled in the present work.

River/Reach	Sediment supply	Flow regime	River/Reach	Sediment supply	Flow regime	River/Reach	Sediment supply	Flow regime	River/Reach	Sediment supply	Flow regime
Big Wood River	Moderate	Snowmelt	Jacoby	Low	Rainfall	Oak Creek	Low	Rainfall	Snake River below Jackson Lake	High	-
Blackmare Creek	Low	Snowmelt	Johns creek	Low	Snowmelt	Pacific creek	High	Rainfall	South Fork Payette	Low/Moderate	Snowmelt
Boise river	Moderate/High	Snowmelt	Little Buckhorn Creek	Low	Snowmelt	Rapid river	Moderate	Rain-on-snow/ Snowmelt	South Fork Red River	Low	Snowmelt
Borgne d’Arolla	High	Glacial fed	Little Granite Creek	Low /Moderate	Snowmelt	Redwood Creek	High	Rainfall	Squaw Creek USGS	Moderate	Snowmelt
Clearwater River	Moderate/High	Impounded	Little Slate	Low	Snowmelt	Saint-Louis Creek	Low	Snowmelt	Sunlight Creek-4	High	Snowmelr
Dollar Creek	Low	Snowmelt	Lochsa Creek	Moderate	Rain-on-snow/ Snowmelt	Sagehen Creek	Low	Snowmelt	Sunlight Creek-11	Moderate/High	Snowmelt
East Fork San Juan	High	Rain-on-snow/ Snowmelt	Lolo Creek	Low/Moderate	Snowmelt	Salmon River below Yankee	Low/Moderate	Snowmelt	Susitna River near Talkeetns	High	Glacial fed
East Saint-Louis Creek	Low	Snowmelt	Main Fork Red River	Low	Snowmelt	Salmon River near Obsidian	Moderate/High	Snowmelt	Susitna River at Sunshine, Alaska	High	Glacial fed
Fool Creek	Low	Snowmelt	Middle Fork	Moderate/High	Snowmelt	Salmon River near Shoup	Moderate	Snowmelt	Talkeetna River near Talkeetna	High	Glacial fed
Fraser River	High	Snowmelt	Middle Fork Piedra River	Low	Rain-on-snow/ Snowmelt	Selway River	Moderate	Rain-on-snow/ Snowmelt	Thompson Creek	Moderate	Snowmelt
Goodwin creek	Moderate	Rainfall	Nahal Yatir	High	Flash-floods	Silver Creek	Moderate	Rain-on-snow/ Snowmelt	Trapper Creek	Low	Snowmelt
Harris creek	Low	Rain-on-snow/ Snowmelt	North Fork Clearwater	Moderate	Rain-on-snow/ Snowmelt	Snake River	Moderate/High	Impounded	Turkey Brook	Low	Flahs-floods
									Valley Creek	Moderate	Snowmelt

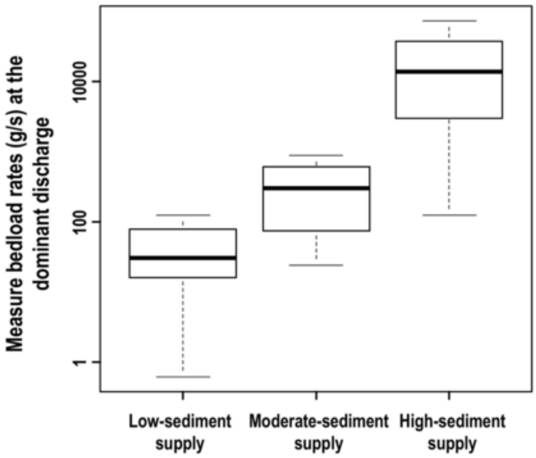

Fig 1. Differences in bedload transport rates according to sediment supply conditions for the sample dataset described in Tables 1 to 3. Sediment supply conditions were defined based on GoogleEarth visual inspection and data provided in the compiled papers The boxes represent the range between the 25th and 75th percentiles, the dark lines the 50th percentile and the whiskers the upper and lower values corresponding to 1.5 times the interquartile range.

The degree of surface coarsening has usually been quantified in fluvial geomorphology through the 'armour ratio' (D_i^*): the ratio between a characteristic grain size (normally, the median size) on the surface GSD and the same characteristic grain size in the subsurface GSD (Bunte and Abt, 2001):

$$D_i^* = \frac{D_{i_s}}{D_{i_{ss}}} \quad \text{Eq. 1}$$

where D_i refers to the ith-percentile of the GSD. Average armour ratios are larger in the compiled field data if estimated using the median size rather than using the D_{84} (~3.1 against ~1.8, respectively) (Fig. 3), outlining that differences between both GSDs tend to be greater if using finer size fractions.

We can observe systematic differences in armour ratios among the different channel morphologies (Fig. 4). In general, multi-thread channels and rivers with riffles and pools exhibit a lower degree of surface armouring, while plane-bed and step-pool channels show higher armour ratios. These differences are statistically significant (Welch's t-test for unequal variances, p-value < 0.05).

The scale of the roughness and protruding elements in step-pool channels are in general larger than other channel types, with channel-spanning ribs (steps) composed by an accumulation of jammed cobbles and boulders transverse or oblique to the channel (Zimmermann and Church, 2001; Chin and Wohl, 2005), alternating with pools (Church and Zimmermann, 2007; Lamarre and Roy, 2008b). Step-pool streams are normally close to headwater areas and are largely associated with the accumulation of fine colluvium inputs into pools and around protruding boulders (Turowski et al., 2011; Recking, 2012; Recking et al., 2012; Piton and Recking, 2017). Accordingly, protruding cobbles and boulders can be found on the bed surface of step-pool channels, even with large sediment supplies and thick alluvial covers. This may explain the generally larger armour ratios observed for step-pool streams. Similarly, the data for braided rivers tend to show lower armour ratios (Fig. 4), which may result from the large sediment inputs typical of braided streams increasing grain mobility and preventing the formation of stable particle arrangements (Hassan et al., 2008, 2020; Venditti et al., 2017). Additionally, braided and riffle and pool systems are typically located in the lower parts of the catchment compared to step pool streams. Consequently, this implies that the formers tend to re-

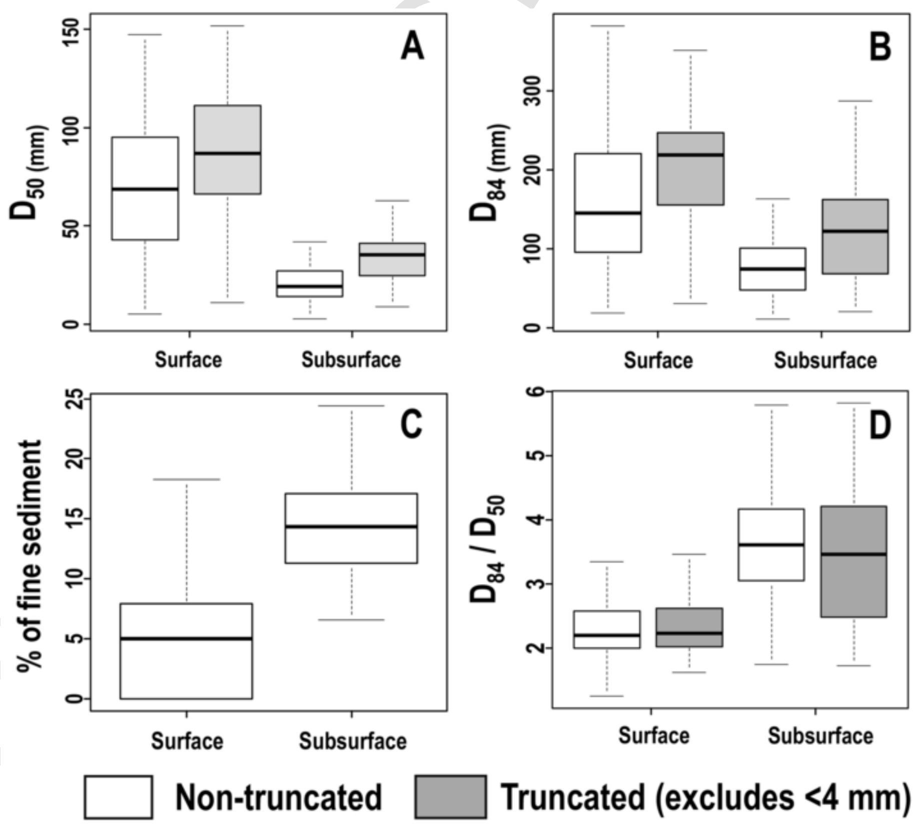

Fig. 2. Comparison between surface and subsurface grain-size parameter distributions in the compiled database. (A) D_{50} (in mm). (B) D_{84} (in mm). (C) Percentage of fines (< 2mm) present in the sediment. (D) D_{84}/D_{50} ratio. The boxes represent the range between the 25th and 75th percentiles, the dark lines the 50th percentile and the whiskers the upper and lower values corresponding to 1.5 times the interquartile range.

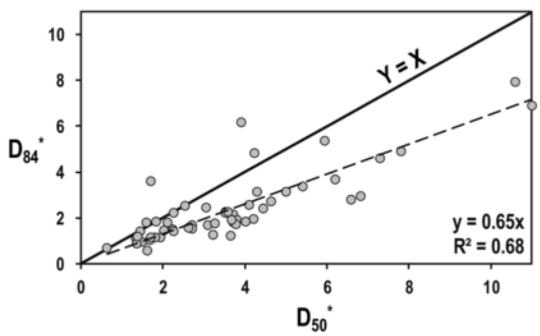

Fig. 3. Comparison between the armour ration based on the 84-th percentile of the GSD (D_{84}*) and the armour ratio based on the median size of the GSD (D_{50}*).

ceive finer sediment loads and be somewhat less prone to develop coarser armours, even if their sediment supply is limited. In this regard, large armour ratios may have some dependence on the upstream/downstream location of the stream and on its geological context, as already suggested by Pitlick et al. (2008).

3.2. Sediment supply and hydrological controls on surface coarsening

Flume experiments suggest a double influence of sediment inputs on surface coarsening. On the one hand, the GSD of the source sediment upstream should exert an obvious control on the grain calibre and the sand content of the available bed material within a specific river reach, which in turn may condition the sediment size of the streambed surface (e.g., Odgaard, 1984; Chin et al., 1994; Marion and Fraccarollo, 1997; Garde et al., 2006; Parker, 2008; Bertin and Friedrich, 2018; Hassan et al., 2020). On the other hand, flume experiments have also shown how the sediment load exerts a primary control on the degree of surface coarsening in gravel-bed rivers (e.g. Dietrich et al., 1989; Hassan et al., 2006).

Within the compiled field data, we observe some statistically significant (p-value = 0.00 < 0.05) and moderate correlation between surface and subsurface GSD (Fig. 5), which supports the hypothesis of the influence of the GSD of the parent bed sediment inputs on the GSD of the streambed's surface. However, it is interesting to notice how variability in the GSD is larger for surface than subsurface GSD (see Figs. 2A and B): the coefficient of variation (ratio between standard deviation and mean) for D_{50} and D_{84} are 62% and 66% in the case of surface GSD, respectively, whereas they are 43% and 52% in the case of subsurface GSD. This suggests that grain-size variability introduced by the sediment supplies is diluted by the variability in surface coarsening introduced by some other controls. In this regard, the compiled data also show some statistically significant differences (ANOVA test, p-value < 0.05) in armour ratios according to our initial classification of the compiled rivers as susceptible to show low-, moderate- and high-sediment supplies (Fig. 6): rivers initially grouped as rivers with potential high sediment supplies tend to show lower armour ratios than streams assumed to have low sediment feeds. This agrees with Dietrich et al., (1989), who reported how surface coarsening develops in flume experiments when there is an imbalance between sediment supply from upstream and the ability of the flow to mobilize the bedload; thus, we could expect an increase in surface armouring with,

decreasing bedload supplies, as Fig. 6 suggests. Nevertheless, some streams that we assumed to have high sediment supply have armour ratios considerably larger than 1-2; and vice versa, some rivers that we assumed to have low sediment supply show armour ratios close to ~1-2. This result could be partially due to misclassification, but also related to the fact that bed texture adjusts to sediment supply not only through surface coarsening, but at the same time, through the development of different bedforms and particle arrangements (Venditti et al., 2017; Hassan et al., 2020).

It is also interesting to note some differences according to the hydrological regime: snowmelt-dominated rivers tend to show coarser surface sizes (see Fig. 5A and 5B) and larger armour ratios (see dotplot shown in Fig. 7A and 7B) than rainfall or flash-flood dominated streams. Furthermore, the percentage of fine sediment also tends to be lower in these snowmelt-dominated streams (Fig. 7C).

On this point, many classical flume experiments on surface coarsening were accomplished under constant water discharge and bedload grain sizes (e.g. Dietrich et al., 1989). However, natural rivers experience very often gradually varied flow hydrographs, and we could expect the amount of entrained bed material and the grain size of the bedload to increase as flow discharge rises (Milhous, 1973; Jones and Seitz, 1980; Kuhnle and Willis, 1992; Andrews, 1994; Lisle, 1995; Wathen et al., 1995; Powell et al., 2001; Ryan and Emmett, 2002; Wilcock and McArdell, 1993, 1997; Clayton and Pitlick, 2008; Ferrer-Boix and Hassan, 2014, 2015; Pitlick et al., 2008; Recking et al., 2016; Vázquez-Tarrío et al., 2019a). In this regard, Hassan et al. (2006) investigated, in a flume, the influence of flow hydrograph on surface armouring, observing varying textural responses to steady vs. gradually varying flows. They compared experimental runs accomplished with a relatively flat and constant hydrograph to those accomplished with sharply peaked hydrograph, obtaining a well-armoured bed surface in the former experimental conditions and an unarmoured bed in the latter. Hassan et al. (2006) considered the first type of experimental conditions as representative of perennial streams subjected periodically

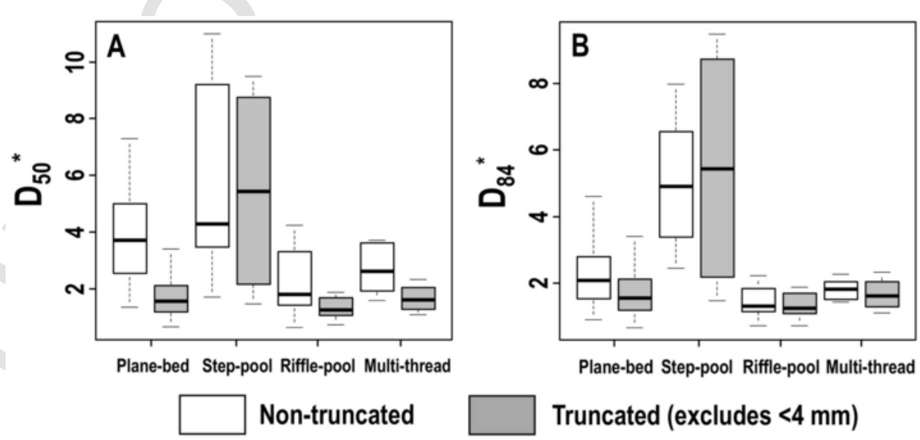

Fig. 4. Distributions of armour ratios according to channel morphology. See main text for more discussion about the differences observed among the different channel morphologies. A: D_{50}*. B: D_{84}*. The boxes represent the range between the 25th and 75th percentiles, the dark lines the 50th percentile and the whiskers the upper and lower values corresponding to 1.5 times the interquartile range. Number of plots: 26 (Plane-bed), 7 (Step-pool), 15 (Riffle-pool) and 7 (Multi-thread)

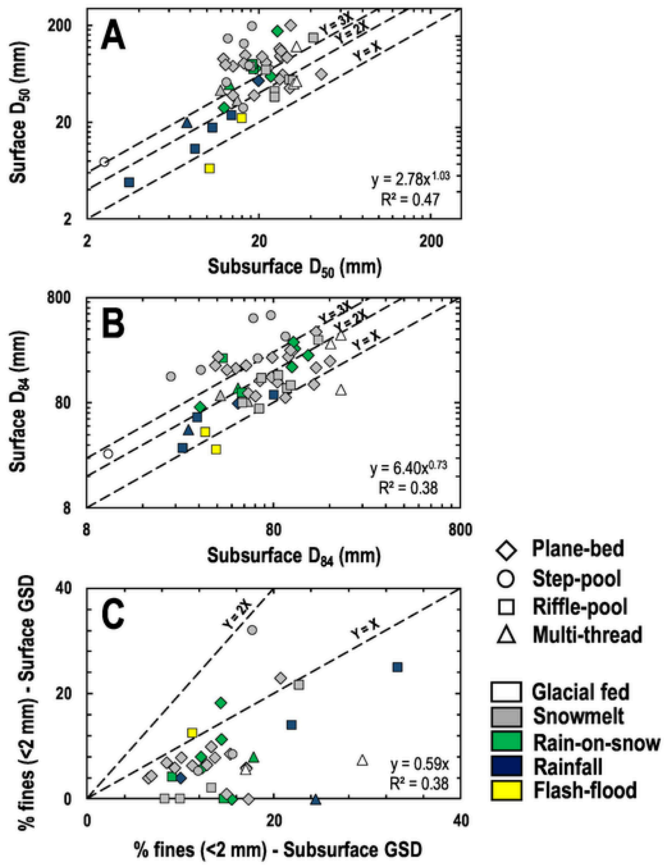

Fig. 5. Surface grain-size parameters plotted versus subsurface parameters. (A) D_{50}. (B) D_{84}. (C) Percentage of fine sediment (< 2 mm). We have segregated the data according to hydrological regime and channel morphology.

to long-lasting floods (e.g. snowmelt). In the opposite extreme, the second type of experimental setting was considered as representative of streams experiencing flash-flood hydrology. More recently, Plumb et al. (2019) also accomplished a series of laboratory experiments to investigate how unsteady flows affect bedload transport in gravel-bed rivers. They conducted several experiments with equal peak discharges and varying duration, and they reported larger armour ratios for longer-duration hydrographs.

We could, thereby, expect differences in mobility between different grain-size classes with fluctuations in flow discharge in natural rivers. Indeed, some of the trends observed with the compiled field data and shown in Figs. 5 and 7 agree with flume experiments exploring the influence of flow hydrograph in surface coarsening. Snowmelt systems tend to show coarser surfaces (Fig. 5) and larger armour ratios (Fig. 7): selective transport and horizontal winnowing of fines during long and sustained recession limbs in snowmelt-dominated streams exhaust the fine sediment and favour the development of a cover of coarse material preventing further sediment transport (Harrison, 1950; Gessler, 1970; Little and Mayer, 1972; Proffitt and Sutherland, 1983; Chin et al., 1994). At the opposite end of the spectrum we find rivers submitted to a flash-flood regime, which typically do not show surface armouring (see Figs. 6 and 7). A flash flood involves a sudden increase of peak flows, bed shear stresses, and equal mobility for all the particle sizes represented in the streambed and the rapid nature of flow recession in these hydrological conditions hinders fine sediment winnowing and surface coarsening (Laronne and Reid, 1993; Laronne et al., 1994; Reid and Laronne, 1995). In such cases, we should not expect large differences between the surface, subsurface, and bedload GSDs. It is also noticeable within the compiled field data that glacial-fed rivers, which are submitted to a hydrology somewhat comparable to snowmelt dominated rivers, show relatively lower armour ratios than snowmelt streams (Fig. 7B). Nevertheless, glacial-fed rivers show larger amounts of fine sediment within the bed material than snowmelt dominated streams (Fig. 7C). In truth, glacial-fed streams have high-sediment supplies from glacial/periglacial sources, i.e. particularly the 'glacial flour' transported from glaciated upland basins. The influx of fine sediments represented by the glacial flour may help the coarse grains composing the armour layer to become more mobile (Cui et al., 2003; Venditti et al., 2010a, 2010b; Yager et al., 2015). In addition, the flow regime of glacial-fed rivers is often characterised by daily peaks of discharge, rising and falling successively, and these somewhat shorter, rapidly changing hydrographs, in conjunction with the abundant fine-sediment supply, could be less prone to promote armouring.

We should also consider that adjustments of the streambed to shifts in sediment supply conditions are not always synchronous and there

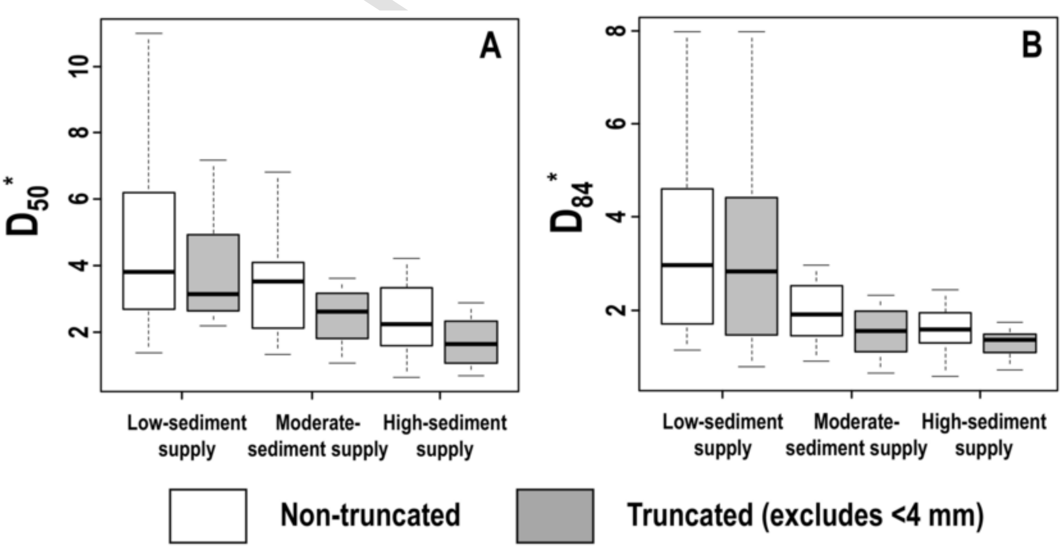

Fig. 6. Distributions in armour ratios according to our classification of the compiled case-studies in terms of sediment supply conditions (mostly based on visual inspection in Google Earth). (A) Armour ratio based on the D_{50}. (B) Armour ratio based on the D_{84}. The boxes represent the range between the 25th and 75th percentiles, the dark lines the 50th percentile and the whiskers the upper and lower values corresponding to 1.5 times the interquartile range. Number of plots: 22 (Low-sediment supply), 17 (Moderate sediment-supply) and 15 (High-sediment supply).

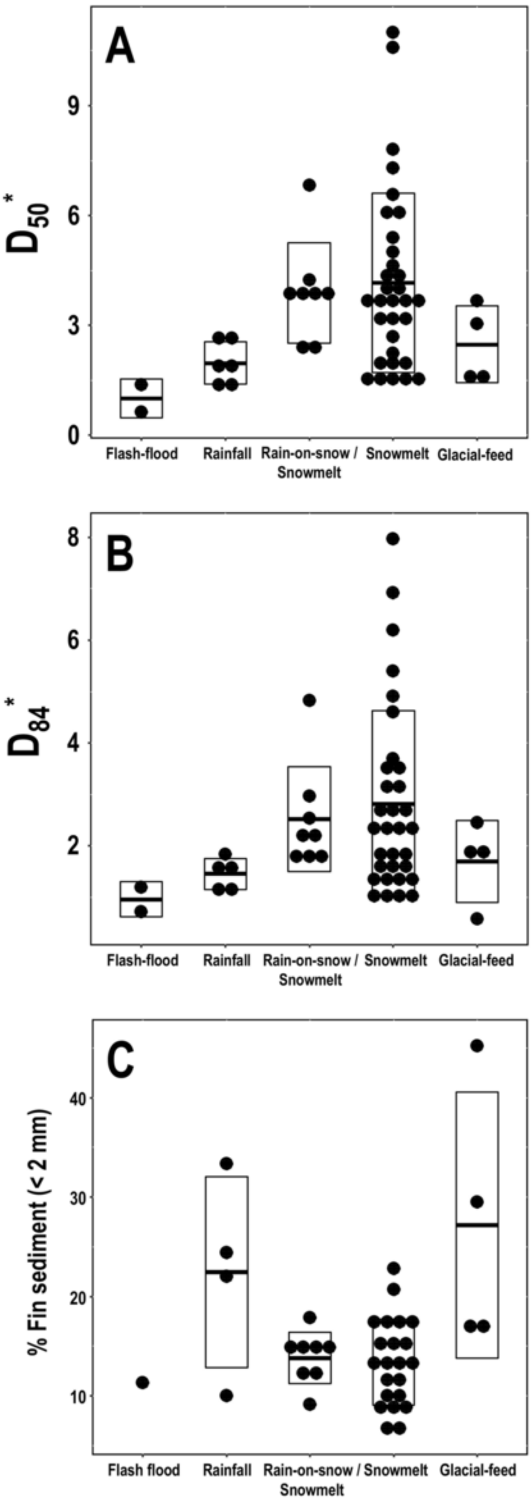

Fig. 7. Differences in armour ratios (A and B) and percentages of fine sediment in the subsurface GSD (C) according to the dominant flow regime. The boxes represent the range between the 25th and 75th percentiles, the dark lines the 50th percentile.

is potentially a lag between the two. Over the long-term, surface coarsening slowly propagates downstream after widespread land-cover changes in the upland basin or downstream from a dam (Rollet et al., 2014), so it can take several years before we observe riverbed coarsening following a significant upstream perturbation. Over shorter time scales, we may observe seasonal changes in sediment supply in gravel-bed rivers that may potentially affect surface armouring. On this point, several authors reported in the field seasonal and inter-annual changes in bedload rating curves (Moog and Whiting, 1998; Hassan and Church, 2001). In glacial-fed or snowmelt systems, for instance, there can be significant bedload transport for a given discharge in early spring, while bedload rates are reduced for similar flow discharges occurring at the end of the melting season (Carrillo and Mao, 2019; Misset et al., 2020). Hence, some hysteresis in bedload supplies can be observed over the hydrological year, so seasonal changes in surface armouring could be expected (Moog and Whiting, 1998). Additionally, some studies have reported riverbed textural ‘memory’ of past flows. For instance, flume experiments by Mao (2018) showed how the occurrence of a high-magnitude flow may reduce the bedload fluxes expected for subsequent long and low-magnitude floods. Similarly, other researchers have suggested some textural dependence on the history of antecedent sub-threshold flows, those flows unable to break up the armour layer but capable of winnowing fine sediment and rearranging particle structures (e.g. Ockelford and Haynes, 2013). In this regard, field observations by Masteller et al. (2019) at the Erlenbach torrent (Switzerland), documented in this small-scale riverbed how particle rearrangements by antecedent low flows are disrupted by the occurrence of large floods. Then, bed conditions show some dependence on the history of previous floods and the time passed after the last large flood episode. Consequently, we believe that all the seasonal and inter-annual variability in hydrological and sediment conditions could explain a significant amount of variability in armour rations within the field data and some overlap between the different hydrological conditions in Figs. 5 and 7.

It should be also mentioned the unavoidable influence of methodological biases, which may explain part of the variability observed in armour ratios. Within the compiled field data (Table 1), surface GSD was generally sampled using a grid-by-number pebble count (Wolman, 1954), while subsurface GSD was always obtained from one variant or another (dredging, digging, frozen cores…) of the bulk volume sampling strategy (Church et al., 1987). It is true that particle-size distributions determined from volume-by-weight (size-sieving of bulk volume samples) and grid-by-number (pebble count) samples are often said to be equivalent (Kellerhals and Bray, 1971; Bunte and Abt, 2001; Rice and Haschenburger, 2004), so this should not cause a large increment in armour variability. However, there are other issues concerning the sampling strategy that are intrinsic to the complex challenge of unbiased sampling of a heterogeneous river reach (e.g. the number of pebble-counts or sub-surface samples, the areal extent, the exact sampled facies, etc) that may differ across the compiled case studies. This should contribute somehow to variability in the available data.

3.3. *Surface coarsening and bedload transport*

As discussed above, larger degrees of surface coarsening are related to low sediment supply and fine sediment exhaustion from the streambed surface. In this regard, apart from armouring, the streambed surface in gravel-bed rivers shows different patterns of structural organization, which goes from imbrications, particle clusters and clast arrangements at the grain and small scales to bed forms, such as stone-cells, transverse ribs, gravel bars or bedload sheets, at the metric/decametric scale. Field observations and flume research (Hassan and Church, 2000) have shown how these bed features evolve with sediment supply (Hassan et al., 2008; Venditti et al., 2017). Hence, surface armouring and bed structures (bedforms, particle clusters, arrangements) tend to coevolve (Venditti et al., 2017), even though Hassan et al. (2020) have recently shown in the flume how particle clusters and clast arrangements can quickly absorb the streambed response to changes in sediment supply, without an equivalent adjustment in the degree of armouring.

There is a large body of field evidence pointing to the large control exerted by surface armouring, clast arrangements and particle clusters on grain stability and particle-entrainment conditions. Early tracer observations by Laronne and Carson (1976) described the influence of particle arrangements on the dispersion of tagged stones. Later, Klingeman and Emmett (1982) reported larger critical shear stresses in the rising than in the falling limb of floods, which they linked to enhanced bed stability by initial armour. In the same vein, a series of field observations at Turkey Brook (England) (Reid and Frostick, 1984; Reid et al., 1985; Reid et al., 1992; Clifford et al., 1992; Reid and Hassan, 1992) suggested an important influence of particle interlocking and particle clusters on increasing thresholds for particle entrainment. Further field research by Church et al. (1998) and Church and Hassan (2002) in Harris Creek (Canada) also pointed to the effects of bed structures (clusters, stone cells) in increasing bed-entrainment threshold stresses. In this regard, field experiments by Wittenberg and Newson (2005), Oldmeadow and Church (2006), and Lamarre and Roy (2008a) also highlighted the importance of particle clusters to modulate and moderate the entrainment of bed material. Later, Turowski et al. (2011) observed in four alpine streams significant correlations between the bed-entrainment threshold discharge for a given flood and the discharge at the end of transport in the most recent event, which they linked to temporal changes in bed structures. More recently, Masteller et al. (2019) reported that significant reorganization of the bed through time (particle arrangments) has a large influence in increasing the thresholds for sediment entrainment in a steep channel from Switzerland.

As with field studies, flume research has also highlighted the important interplays between particle arrangements/clusters and streambed mobility. Early flume experiments by Brayshaw et al. (1983) already indicated how particle clusters tend to increase the stresses required to move surface particles. Later flume experiments by Church et al. (1998) and Hassan and Church (2000) found an increase in bed stability introduced by particle clusters. More recently, a series of flume experiments indicated that the development of particle arrangements and clusters after prolonged interflood periods of sub-threshold flow increases bed stability (Monteith and Pender, 2005; Paphitis and Collins, 2005; Haynes and Pender, 2007; Ockelford and Haynes, 2013; Ockelford et al., 2019). In this regard, Mao (2012) observed contrasts in sediment entrainment before and after the peaks of hydrographs in flume experiments, which he related to a change in the organization of the streambed surface (i.e. increased particle clusters). More recently, Perret et al. (2020) compared experimental runs with a quasi-flat bed to runs with alternate bars), and observed significant differences in bed stability.

According to this previous literature, we could then expect some covariation between grain mobility and armour ratios in the compiled field data. To explore this issue, we analysed the values for the 'transport stage' ratio (τ_d^*/τ_c^*) at the dominant channel-forming flow in each one of the selected case studies, i.e. the ratio between the peak bed shear stress at the dominant discharge (τ_d^*) and its critical value (τ_c^*) for incipient sediment motion. Values of this parameter were retrieved from the supplementary information provided by Mueller et al. (2005) and Phillips and Jerolmack (2019) for 39 of the compiled field cases. In five of the remaining case studies (Goodwin creek, Harris creek, Jacoby, Susitna river near Talkeetns, Trapper creek) we determined transport stages parameter based on the available bedload discharges; we considered as τ_c^* the median value of Shields stress at which the dimensionless transport rates (W^*) intersect a reference transport rate of $W^* = 0.002$ (Parker, 1990), as:

$$W^* = \frac{1.65 \bullet g \bullet q_{sv}}{\left(\frac{\tau}{\rho}\right)^{3/2}} \qquad \text{Eq. 2}$$

where g is gravitational acceleration, ρ is water density, q_{sv} is the volumetric unit bedload discharge and τ is the bed shear stress:

$$\tau = \rho \bullet g \bullet S \bullet d \qquad \text{Eq. 3}$$

where S is the bed slope and d the flow depth, which was estimated here based on flow discharge and the Rickenmann and Recking (2011) fit to Ferguson's (2007) friction law. Shields stresses at the dominant discharge were computed as:

$$\tau_d^* = \frac{\tau_d}{1650 \bullet g \bullet D_{50}} \qquad \text{Eq. 4}$$

where τ_d is the bed shear stress at the dominant discharge. In the remaining five case studies (Borgne d'Arolla, Nahal Yatir, Snake river below Jackson Lake, Sunlight Creek and Susitna river at Sushine) transport stages could not be defined due to lack of good data.

In general, well-armoured ($D_{84}^*>3$) streams show lower transport stages at the dominant discharge than poorly armoured ($D_{84}^*<2$) rivers (Fig. 8A). Nevertheless, there is some overlap between the different groups, particularly with the group of moderately-armoured reaches ($2 < D_{84}^* < 3$). This variability could be explained by the fact that streambed mobility is not only controlled by grain size, but also by particle shapes, imbrications and orientation (Gomez, 1993, 1994; Kirchner et al., 1990; Buffington et al., 1992). Also, as Hassan et

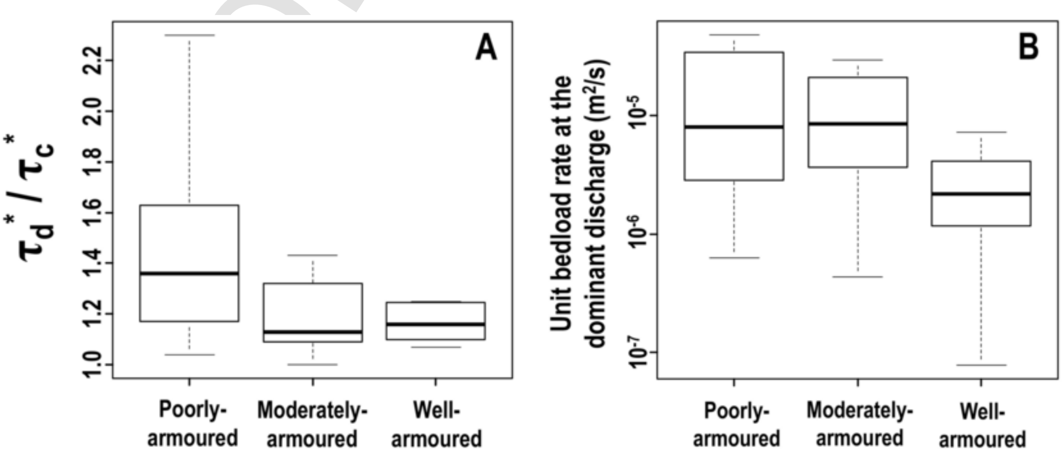

Fig. 8. (A) Transport stages and (B) bedload rates at the dominant discharge in poorly armoured ($D_{84}^*<2$), moderately armoured ($2< D_{84}^* < 3$) and well armoured ($D_{84}^*>3$) rivers. The boxes represent the range between the 25th and 75th percentiles, the dark lines the 50th percentile and the whiskers the upper and lower values corresponding to 1.5 times the interquartile range. Number of plots: 30 (poorly armoured), 12 (moderately armoured) and 13 (well armoured).

al. (2020) suggested, changes in bed structures (clusters, cells, transverse features) can occur with minimum changes in armouring.

Considering the control exerted by bed structures on grain stability and particle entrainment, we could also expect differences in bedload rates according to differences in clast arrangements, particle clusters and armouring (Hassan et al., 2008). Indeed, the experimental results found by Church et al. (1998) and Hassan and Church (2000) pointed to lower sediment transport over a structured riverbed than over a non-structured riverbed. In this regard, the previously mentioned field experiment carried out by Oldmeadow and Church (2006) reported greater sediment transport in an unstructured reach compared to a reference structured reach. Similarly, other field researchers have documented high bedload rates after large floods in step-pool channels after step-pool destabilization, due to an increase in mobility of larger grains (Gintz et al., 1996; Lenzi et al., 1999; Lenzi et al., 2004; Turowski et al., 2009; Vázquez-Tarrío et al., 2019b). In addition, recent flume experiments by Plumb et al. (2019) and Perret et al. (2020) (comparing the bedload behaviour of different bed configurations) reported differences in bedload rates according to differences in bed texture. In this regard, the compiled field data confirm larger bedload rates in poorly armoured compared to well-armoured streams, as flume experiments suggest (Fig. 8B).

4. Meta-analysis on the compiled data

4.1. General aim

The previous review highlights how a long tradition of field and flume research has largely confirmed the existence of close links between sediment supply, channel morphology, bedload transport, and streambed texture in gravel-bed rivers. This idea, which has been present in fluvial geomorphology and river morphodynamics for many decades (e.g. Lane, 1955b), is supported by our systematic review of a wide database of field studies compiled from the scientific literature on fluvial bedload transport. However, field data also show an important scatter, so some questions remain open concerning how to interpret armour ratios measured in the field in terms of sediment supply and whether (or not) quantitative relations between bedload fluxes, surface armouring, and channel morphology could be extracted from the scattered available bedload information.

Most of the research done to date in flumes has been accomplished with the planform fixed (Lawson, 2020) and/or under constant or nearly constant flow discharge (Hassan et al., 2006). This begs the question if the quantitative trends inferred from flume studies could be extrapolated to natural rivers with varying flow hydrographs and episodic sediment supplies. Bearing all this in mind, we accomplished a meta-analysis of the compiled field data with two main goals: i. seeking for the quantification of any potential trend between armour ratios and bedload fluxes within the available bedload field information; and ii. explore the relative weight of sediment supply versus hydrological controls on variability in surface armouring.

4.2. Materials and methods

In a first step, we analyzed how armour ratios evolve with changes in sediment-supply conditions in natural rivers. In this regard, Dietrich et al. (1989) reported how armour ratios increase while sediment feed decreases compared to the overall bedload transport capacity of the channel, in flume experiments. To explore these linkages, they proposed their own metric, the dimensionless transport rate ratio, (q^*). This parameter was initially defined by Dietrich et al. (1989) as '*the transport rate for the coarse surface layer normalized by the transport rate for a surface as fine as the sub-surface or load*'; that stated:

$$q^* = \frac{q_{s_s}}{q_{s_{ss}}} \qquad \text{Eq. 5}$$

where q_s refers to the bedload transport rate per unit width of channel and the subscripts *s* and *ss* to the surface and subsurface sediment, respectively. According to Dietrich et al. (1989), q^* '*should be unity when sediment supply rate matches the river's ability to transport the load and should decrease towards 0 as the surface coarsens when supply is reduced'*. Thus, they hypothesized that a survey of rivers to determine q^* may provide a quantitative method to determine the sensitivity of rivers to changes in sediment supply (for example, after major land-use modifications). Aiming to test this hypothesis, we computed the q^* ratio for the compiled field data. For the numerator in eq. 5 we used the bedload rates at the dominant channel-forming discharge. Doing so, we assume that bedload rates at the dominant discharge provide a good proxy of sediment supply from upstream. Bedload rates at the dominant discharge were obtained from the available bedload rating curves for each study case. The denominator in eq. 5 (q_{ss}) was estimated based on flow characteristics at the representative channel-forming discharge and the subsurface GSD. We thereby assume a correspondence between the long-term averaged bedload and subsurface GSD distributions, which is often postulated for the GSD of the bedload (Church and Hassan, 2005; Vázquez-Tarrío et al., 2019a). We used Rickenmann and Recking (2011) formula for computing water depth (and shear stresses) from dominant discharges, and Recking's bedload equation (Recking, 2013a, 2013b; Recking et al., 2016) for bedload computation (the two steps based on subsurface GSD). There are three main advantages of choosing this bedload formula. First, this equation is continuous and describes with a single expression the transition from partial to full mobility conditions. Second, it incorporates an explicit correction of channel morphology in reference threshold Shields stresses, which accounts for differences in the shear stress distribution with dominant macroforms, such as step-pools or riffle and pools (Recking et al., 2016). Finally, this equation has been tested and validated against bedload discharge information from natural gravel-bed rivers (e.g. Hinton et al., 2018), including the field cases considered in this paper.

Based on dimensional analysis of Yalin's (Yalin, 1972) bedload transport equation, Dietrich et al. (1989) deduced an expression linking surface armouring (D_{50s}/D_{50ss}) and q^*. Similarly, here, based on the dimensional analysis of Recking's (2013b) equation (after Recking et al., 2016), we derived two different expressions (see details in the supplementary information) for the links between armour ratios and q^*:

$$D^*_{84} = f \bullet {q^*}^{-\frac{1}{5}} \text{ for partial} - \text{mobility conditions} \qquad (6)$$

$$D^*_{84} = {q^*}^{-1} \text{ for full} - \text{mobility conditions} \qquad (7)$$

where f in eq. 6 is a parameter relating D_{50^*} to $D_{84}{}^*$, i.e. the slope in Fig. 3 (~0.65). Then, we compared the trends observed within the compiled data with those expected from Eqs. 6 and 7. Additionally, we compared the results derived from field data with those from previous flume experiments that explored the effect of reductions in sediment feed on the surface texture (Church et al., 1998; Hassan and Church, 2000; Nelson et al., 2009). Table 4 describes the main characteristics of these experiments. Information for these flume investigations was extracted from graphics presented in Venditti et al. (2017) (Figs. 16.1, 16.2 and 16.5 in that paper). Venditti et al. (2017) estimated q^* for these flume experiments as the ratio between the bedload transport rate after the bed has adjusted to a new sediment feed divided by

Table 4
Sources of flume data compiled for this study. *S:* Flume slope. *W*: Flume width. *L*: Flume length. *h*: water depth. D_{50}: 50-th percentile of sediment GSD. *r*: experiment duration.

Flume	Source	S	W (m)	L (m)	h (cm)	D_{50s} (mm)	Shields	Feed rate	r (h)
Tsukuba	Nelson et al. *(2009)*	0.0035-0.0052	7.5	0.3	10.2-11.3	3.7-4.9	0.049-0.086	1.7-17.4g/min·cm	6-7.5
Berkeley	Nelson et al. *(2009)*	0.0043-0.0055	28	0.9	21.8-22.8	10.1-11.8	0.045-0.061	0-23.3 g/min·cm	20.7-28.9
UBC	Church et al. *(1998)*	0.001-0.012	0.5/0.8	6/10	0.5-7.4	1.9-5.1	0.003-0.117	No feed	-
UBC	*Hassan and Church (200)*	0.006/0.007	0.8	10	0.1-6.7	2.4-4.5	-	1.2-0.644 kg/h	96

the transport rate for the initial unarmoured bed, before any feed reduction.

Moreover, the dimensionless sediment transport ratio q^* is an equivalent parameter to the bedload transport rate efficiency (e), as defined by Bagnold (1966):

$$e = \frac{q_{sv} \bullet (\rho_s - \rho) \bullet g \bullet tan\varphi}{\omega} \tag{8}$$

where ρ_s is the density of sediment (~2650 kg/m^3), φ is the friction angle of the bed material (we assumed ~52°, following Buffington et al., 1992 and Recking, 2012) and ω is the specific streampower:

$$\omega = \frac{\rho \bullet g \bullet S \bullet Q}{w} \tag{9}$$

where S is the bed slope, Q the water discharge and w the channel width. This transport efficiency parameter represents the ratio between the actual bedload rates and the total amount of stream power available in the study reach, i.e. it provides an idea of the fraction of stream power used in bedload transport, which is in general very small. One advantage of the bedload transport efficiency parameter compared to q^* is its independence in the choice of a bedload function. Consequently, we also computed bedload transport efficiencies at the dominant discharge for each study case and we analyse the correlation between armour ratios (D_{84}*) and bedload transport efficiencies e. It should be noted that, according to Fig. 5B, there is some nonlinear dependence between surface D_{84} and the GSD of the parent bed material. In order to remove this effect from the regression analysis between D_{84}* and e, we employed a corrected version of the armour ratio (D_{84}**):

$$D_{84}^{**} = \frac{D_{84_s}}{D_{84_{ss}}{}^{\beta}} \tag{10}$$

where β is the exponent of the power function relating D_{84s} to D_{84ss} (0.73 in Fig. 5B).

Moreover, if surface armouring coevolves with bedload supplies (e.g. Dietrich et al., 1989; Montgomery and Buffington, 1997), we could also expect some correlation between bedload rating curves and surface armouring. So, in a second step, we did an exploratory analysis of the bedload rating curves available for the selected case studies, in order to investigate the relative amount of variance in bedload fluxes which could be linked to flow strength and bed texture. To do so, we took the available information on bedload discharges (Table 1) and performed a simple regression analysis between bedload intensity and flow strength, which was quantified as the ratio between the peak discharge for each bedload sample and the dominant discharge (hereinafter called flow ratio):

$$\phi = a \bullet \left(\frac{Q}{Q_d}\right)^b \tag{11}$$

where a and b are the intercept and exponent of the regression model, Q/Q_d is the ratio between the peak discharge for the transport episode and the dominant discharge (hereinafter called flow ratio), and ϕ is bedload transport intensity, estimated from:

$$\phi = \frac{q_s}{\sqrt{1.65 \bullet g \bullet D_{84}^2}} \tag{12}$$

Subsequently, we performed a multiple regression analysis linking bedload intensities to both flow and armour ratios:

$$\phi = a \bullet \left(\frac{Q}{Q_d}\right)^b \bullet \left(D_{84}^*\right)^c \tag{13}$$

where c is again an empirical exponent. Nevertheless, the wide diversity of channel morphologies represented amongst the compiled data should be highlighted, since channel macroforms control flow and sediment transport patterns, which in turn may potentially affect 1D relations for bedload rates (Ferguson, 2003; Camenen et al., 2011; Francalanci et al., 2012; Recking et al., 2016; Vázquez-Tarrío et al., 2019b; Vázquez-Tarrío and Batalla, 2019). For this reason, we also introduced a set of three binary indicators into the regression analysis to incorporate the influence of channel morphology:

$$\phi = a \bullet \left(\frac{Q}{Q_d}\right)^b \bullet \left(D_{84}^*\right)^c \bullet e^{d \bullet RP} \bullet e^{e \bullet SP} \bullet e^{f \bullet BR} \tag{14}$$

where RP, SP and BR are the dummy variables taking a value of 1 in the cases of riffle and pool, step-pool and braided channels, respectively. In the case of plane-bed channels, the three dummy variables would be 0. To test whether Eqs. (13 and (14 fit the available bedload information, we used ordinary multiple regression in linearized form and stepwise procedures, after log transforming all the variables included in the equation. With the progressive incorporation of the different independent variables (flow strength→armouring→morphology), we aimed to understand how the percentage of explained variance in bedload rating curves increases when incorporating surface armouring and channel morphology into the regression. To quantify the change in explained variance, we evaluated the values of the adjusted-R^2 regression model coefficients. Additionally, to better assess the relative importance of each independent variable, we used the method proposed by Lindeman et al. (1980), often recommended for assigning shares of relative weight of predictors to the R^2.

4.3. Results

There is a linear and positive correspondence between the dimensionless sediment supply ratio q^* and the bedload transport efficiency e (Fig. 9), which supports the idea that they are two equivalent parameters, quantifying the ratio between actual bedload fluxes and channel bedload transport capacities. Additionally, our initial classification of the selected streams as susceptible to show low-, moderate- and high-sediment supply is in good agreement with the q^* values, so our subjective classification, the sediment supply ratio q^* and transport efficiencies reinforce each other as proxies for sediment supply conditions.

We observe a decreasing trend in armour ratios (D_{84}*) with q^* (Fig. 10A), as Dietrich et al. (1989) described for flume experiments. The obtained fit is very close to the curve defined by Eq. 6 (low-transport stage conditions). This suggests that partial mobility conditions

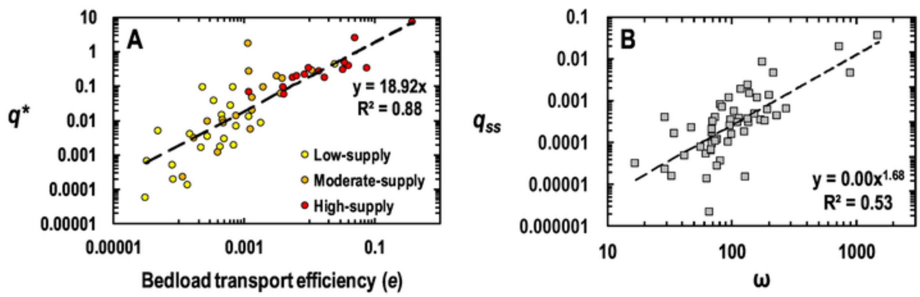

Fig. 9. (A) Dimensionless bedload ratio q^* plotted versus the bedload transport efficiency, at the dominant channel forming discharge. (B) Bedload transport capacities estimated based on the subsurface GSD and Recking's (2013) bedload equation, plotted versus the specific stream power, at the dominant discharge.

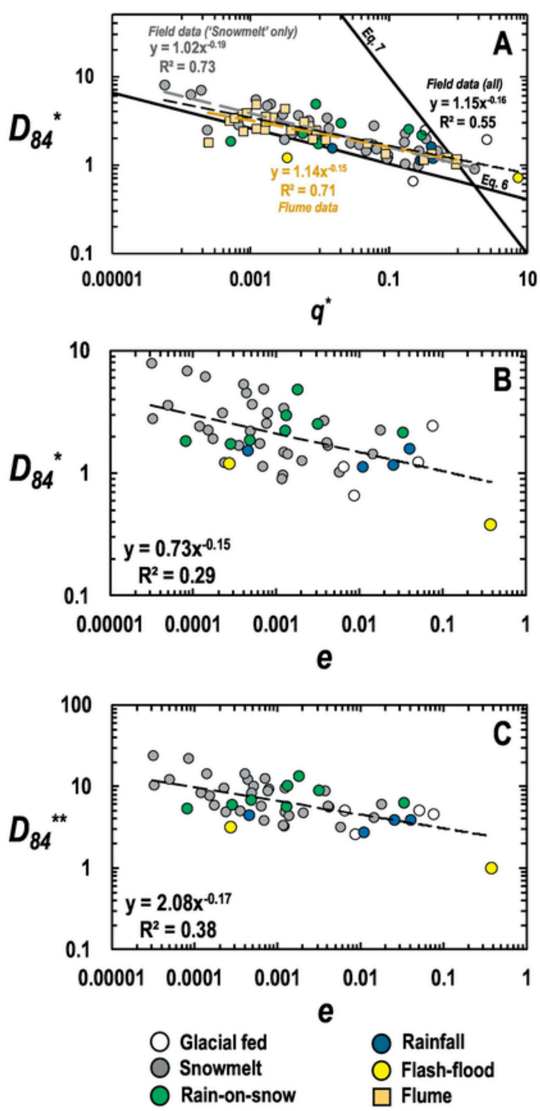

Fig. 10. (A) Armour ratio plotted against the q^* parameter. Flume data were extracted from Venditti et al. (2017). (B) Armour ratio plotted versus the bedload transport efficiency parameter. (C) Corrected armour ratio, plotted versus the bedload transport efficiency parameter. See main text for details.

may dominate bedload motion at the dominant discharge in gravel-bed streams. In addition, we have also incorporated into the plot data from flume experiments (extracted from Venditti et al., 2017; see supplementary information), which tend to overlap the field data: thus, armour ratios change with bedload supply following a similar trend in flume and field data. Similarly, we observe a comparable decreasing trend in armour ratios with bedload transport efficiencies (Fig. 10B and 10C). Additionally, in all cases (flume, field data) we report a similar ~0.15-0.2 power scaling between the armour ratios and the dimensionless bedload q^* ratio or the bedload transport efficiency e. In Table 5 we summarize the root mean square error (RMSE) of the regression analysis for each hydrological regime. This analysis indicates lower variability in armour ratios in rainfall streams compared to snowmelt or glacial-fed systems. This could be related to the larger seasonal and interannual variability in sediment supply in the latter compared to the former.

The R^2 of the best regression fits between q^*, e and D_{84}^* suggests that ~40-50% of the variability in surface armouring in the compiled data could be attributed to differences in the balances between sediment supply and the channel's transport capacity. However, there remains a certain amount of scatter in the plot, which highlights that variability in armour ratios exists with a given sediment supply. That said, this analysis can identify rivers that are more or less armoured than the streambed conditions expected for an 'average behaviour' with a given bedload input. The larger scatter in field ($R^2 = 0.55$) compared to flume data ($R^2 = 0.71$) supports the hypothesis that differences in the hydrological regime could partially explain this variability. To evaluate this scatter, we performed a quantile regression analysis and plotted the regression between the different percentiles of the D_{84}^* distribution and the sediment supply metrics (q^*), obtaining a diagram that illustrates the likelihood of a given value of D_{84}^* with a given sediment supply (Fig. 11).

The variability in armour ratios with a given value of q^*, illustrated by regression models from the 1-st to the 99-th percentiles, could be linked to a set of factors, which include differences in the hydrological regime, seasonal variability in sediment supply and time passed after significant shifts in upstream sediment inputs. For instance, although the number of points is not well balanced across the different groups of data, it is worth pointing out how in Fig. 10A to C data from snowmelt streams tend to plot in the upper envelope of the point cloud and, conversely, data from flash-flood dominated streams tend to fall in the lower envelope, while rainfall dominated rivers project in the middle of the point cloud.

Concerning the analysis on how bedload fluxes correlate to flow strength, surface coarsening, and channel morphology, regres-

Table 5
Root mean square errors (RMSE) for the regression analysis shown in Fig. 10.

Group	N	RMSE		
		D_{84}^* vs q^*	D_{84}^* vs e	D_{84}^{**} vs e
Flash flood	2	1.71	1.37	5.43
Glacial-fed	4	0.96	0.96	1.73
Rain-on-snow/Snowmelt	8	1.37	1.39	4.10
Snowmelt	32	1.04	1.66	4.22
Rainfall	6	0.39	0.42	1.64

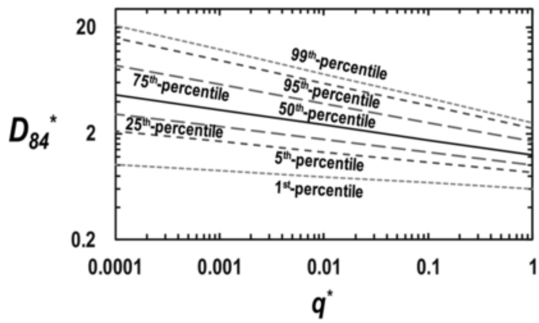

Fig. 11. Diagrams issued from quantile regression analysis of the compiled data, defining the likelihood of a certain value of the armour ratio according to q^*-metrics (see main text for more details).

sion analysis shows that the three considered variables explain the variance in the compiled bedload data to a statistically significant degree (Table 6). The change in R^2 values with the progressive incorporation of the different variables is statistically significant, implying that Eq. (14 is more robust than Eq. (13 (adjusted-R^2 = 0.56 vs. 0.41, respectively) and both are more robust than Eq. (11 (R^2 = 0.08). This supports the existence of some morphological and textural (armouring) imprint on bedload transport rates.

According to the regression model, transport intensities increase with the ~1.7 positive power of flow ratios. Conversely, bedload rates are negatively correlated to armour ratios, i.e. bedload rates tend to be considerably weaker in well-armoured channels. The analysis of the relative weight of each independent variable to the R^2 suggests that flow magnitude is the variable that explains the largest amount of variability in bedload data (~23 % of variance), followed by channel morphology (21% of variance) and armour ratios (12% of variance). Thus, differences in dominant channel morphology have a strong effect on the variability in bedload rates observed between the compiled data, but differences in surface armouring also have a non-negligible influence. Both surface armouring and planform morphology result from the adjustment of grain and macro-roughness, respectively, to the balances between sediment supply and transport capacity, i.e. the self-adjustment of channel roughness in order to maximize bed resistance and minimize the imbalances between the imposed boundary and critical threshold stresses (Dietrich et al., 1989; Lawson, 2020). Consequently, the fitted Eq. (14 quantifies how the increase in bedload rates with flow discharge is modulated by grain and macro-form roughness, which are parameterised through the armour ratio and the dummy variables (i.e. dominant channel type) and are likely largely dependent on sediment supply (e.g. Dietrich et al., 1989; Buffington and Montgomery, 1999a, 1999b).

Table 6
Results from the multiple regression model based on Eq. (8 (see main text).

Variable	Coefficient	Standard Error	t	*p-value*	VIF[1]
Intercept	2.910x10^{-5}	0.074	-140.655	0.000	
Q/Q_d	1.677	0.031	54.207	0.000	1.068
D_{84}^*	-2.266	0.068	-32.998	0.000	1.699
BR	1.827	0.258	7.079	0.000	1.143
RP	2.876	0.072	40.125	0.000	1.151
SP	1.283	0.110	11.659	0.000	1.409

Residual standard error: 2.142 on 4851 degrees of freedom
Multiple R^2 = 0.56; Adjusted R^2 = 0.56; Predictive R^2 = 0.56
F-statistic: 1247 on 5 and 4851 degrees of freedom. *p-value* = 2.2 x 10^{-16}

[1] Variance Inflation Factor

5. Discussion

5.1. General discussion

Surface coarsening is a major textural feature in gravel-bed rivers that has long been studied by fluvial scientists. Our systematic review of previous literature conflates the results from cumulated field and flume research into showing how streambed in gravel-bed rivers responds to a decrease in bedload supply through channel narrowing and a general surface coarsening (Dietrich et al., 1989; Nelson et al., 2009). Hence, the degree of the latter may provide, in principle, an indicator of the dominant sediment supply conditions of a given river reach (Dietrich et al., 1989; Sklar et al., 2009; Venditti et al., 2017) and therefore, it is not surprising that fluvial geomorphologists have often used the field observation of surface coarsening as a way to characterize streambed mobility and/or to diagnose the magnitude of bed degradation below dams, for example (e.g. Rollet et al., 2014; Vázquez-Tarrío et al., 2019c).

The in-depth analysis of a large amount of field data, accomplished here, showed a decline in armour ratios with increasing bedload supply in relation to the channel's transport capacity (quantified through the q^*- or e-metrics), which is similar to trends observed in previous flume experiments (Dietrich et al., 1989; Venditti et al., 2017). Consequently, the overall picture of field data illustrates how the signal linked to differences in sediment supply is a dominant one and is globally well-recorded through the scaling between armour ratios and bedload fluxes. However, disparities in the patterns of sediment supply variability (e.g. at an annual, seasonal or intra-flood scale) among different hydrological contexts complicate the interpretation of surface coarsening measured in the field. For instance, rivers experiencing long-lasting and sustained floods tend to exhaust fine sediment from the riverbed, which in turn enhances the degree of coarsening compared to the situation expected in streams with comparable sediment supply but submitted to sharper and shorter hydrographs. The hydrological regime is then a source of variability in surface coarsening that overlaps the signal related to the dominant sediment supply conditions. In addition, sediment supply is accommodated not only through surface coarsening, but also through adjustments in planform morphology, channel geometry, and clast arrangements, which constitute different degrees of freedom in gravel-bed rivers that change independently from each other (Lawson, 2020; Hassan et al., 2020).

For many applications (channel-design, river restoration), an adequate diagnosis of the hydro-morphological status of a given reach is fundamental. As information on bedload fluxes is lacking in many cases, GSDs and armour ratios measured in the field are often used for a quick characterization of the sediment supply conditions and streambed mobility of those river reaches and to diagnose the bed state after human interventions. However, the observed variability in surface armouring with a given sediment flux may complicate the applicability of armour ratios for these purposes. In this regard, based on quantile regression analysis, we have created a diagram illustrating the likelihood of a certain armour ratio for a given sediment supply in the compiled data (Fig. 11). We believe this empirical diagram could potentially provide an empirical framework for more consistent interpretations (in terms of streambed state and mobility) of armour ratios measured in the field, by combining this diagram with other qualitative knowledge and field information about the dominant hydrological and sediment regime. For instance, the combination of Fig. 11 with some information about the degree of altered flow regime may help to interpret the armour ratios measured downstream of dams. In this regard, for a given sediment reduction, we should expect a more conspicuous coarsening of the streambed downstream of a dam not disturbing the frequency of channel-forming flows (thus, values over the 50-th percentile in Fig. 11), compared to (for example) a run-of-river dam diverting a significant amount of flow and decreasing the frequency of sediment evacuation (thus, values closer to the lower percentile lines in Fig. 11).

5.2. Armour ratio: a proxy for multi-scale streambed configuration?

The review of previous literature presented here, as well as our meta-analyses of a broad database of bedload data, illustrates how planform style, channel geometry, streambed mobility, grain size, and bedload fluxes covary together in gravel-bed rivers. On this point, it has been a tacit idea in fluvial geomorphology that gravel-bed rivers self-organize as to maximize flow resistance (Lawson, 2020), reducing the differences between the imposed boundary and critical bed shear stresses (Dietrich et al., 1989) and adjusting their channel-shape so that dominant floods slightly exceed the critical shear velocity needed to transport bed sediment (Parker, 1978; Phillips and Jerolmack, 2016, 2019). Apparently, this seems to happen in gravel-bed rivers independently of other climatic, tectonic, and lithologic controls (Phillips and Jerolmack, 2016). Consequently, understanding how riverbed mobility (Pfeiffer and Finnegan, 2018), channel-form (Phillips and Jerolmack, 2016; Phillips and Jerolmack, 2019), bed features (Venditti et al., 2017), and planform morphology (Buffington and Montgomery, 1999a, 1999b) are coupled in gravel-bed channels is a key, but evasive, question for predicting river response to external perturbations, such as dams (e.g. Schmidt and Wilcock, 2008; Dade et al., 2011), extreme flood events, land use practices, environmental change, and general landscape evolution.

Data handled in the present manuscript show how section-averaged bed shear stresses, estimated at the dominant channel-forming discharge, are close to the critical thresholds (~1-1.4 times τ_c*) for entrainment of the coarser fraction of bed sediment in well-armoured streams (Fig. 7A). This observation reflects the streambed adjustment to dominant hydraulic conditions and is consistent with decades of theoretical work and field observations supporting the hypothesis of near-threshold gravel-bed channels (Parker, 1978; Parker, 1979; Parker, 2004; Mueller and Pitlick, 2005; Parker et al., 2007; Phillips and Jerolmack, 2016; Métivier et al., 2017; Dunne and Jerolmack, 2019; Phillips and Jerolmack, 2019) and the adjustment of channel geometry in such a way that thresholds for motion of median-size grains occur close to bankfull flows. However, in the compiled field data, Shields stresses can be well above these critical values in the case of poorly armoured streams, which show in general larger bedload fluxes. Pfeiffer et al. (2017) already observed that only supply-limited streams meet the near-threshold channel condition, while in capacity-limited systems they reported Shields stresses at bankfull considerably over the critical levels. Thus, they concluded that the common observation of near-threshold gravel-bed channels simply reflects the fact that most surveyed channels are subject to modest sediment supplies. Nevertheless, we propose an alternative interpretation. According to the data analysed in this manuscript, poorly armoured systems correspond mainly to multi-thread and riffle-pool streams (Fig. 4). These kinds of settings are characterized by complex bar morphologies (Ferguson, 2003) and patterns of grain size sorting (Paola, 1989; Lisle and Hilton, 1992), thus a great variability in shear-stress distributions across their cross-section (Ferguson, 2003; Recking, 2013a; Francalanci et al., 2012; Recking et al., 2016). Consequently, we expect larger variability in bedload estimates when averaging shear stresses across the cross section of these streams (Recking, 2013a). Therefore, it is probable that 1D averaged shear stresses are not an adequate proxy for the actual variability in shear stresses acting at local and grain scales in riffle and pool and multi-thread settings. This may explain the observed deviation from near-threshold conditions, which could be to a large degree an artefact resulting from the assumptions made when estimating cross-section averaged shear stresses (Yager et al., 2018).

Moreover, we also observed how dominant channel morphology modulates the correlation between the bedload rating curves and surface armouring (Table 5). All these trends therefore point to the fact that planform style, dominant macroforms, and grain size adjust together to dominant sediment-supply conditions in natural rivers. In this regard, a typical sequence of reach types observed in many mountain basins corresponds to a downstream progression from step pool at headwaters, plane-bed (or forced pool-riffle) to pool-riffle and/or multithread channel morphology at the piedmont valley (e.g. Warburton, 2007). In their seminal paper, Montgomery and Buffington (1997) suggested that this kind of longitudinal sequence describes opposing trends between sediment supply and transport capacities in the downstream direction. In this regard, Pitlick et al. (2008) documented a trend toward lower armour ratios in downstream reaches of rivers from Colorado and Utah.

Additionally, gravel-bed rivers exhibit a wide diversity of bed features that are larger than individual clasts and smaller than reach-scale patterns. Sediment supply plays a critical role in the development of these bed structures (Buffington and Montgomery, 1999a; Venditti et al., 2017.). Dominant bedforms in gravel-bed rivers evolve from gravel dunes (Carling, 1999) and bedload sheets in poorly armoured streams (Whiting et al., 1988; Nelson et al., 2009; Recking et al., 2009), to a sequence of pebble clusters (Brayshaw, 1984), transverse ribs (Koster, 1978; Allen, 1984), stone lines (Laronne and Carson, 1976) and reticulate stone cells (Church et al., 1998; Hassan and Church, 2000) with decreasing sediment supply (Venditti et al., 2017). Indeed, the stability of a gravel streambed is increased by the presence of particle arrangements and clusters (e.g., Reid and Frostick, 1984; Church et al., 1998; Hassan and Church, 2000; Piedra et al., 2012; Ockelford and Haynes, 2013; Heays et al., 2014). Therefore, streambed textures adjust to reduction in sediment supply not only through surface coarsening, but also through a decrease in streambed mobility and a change in bed surface organization. Venditti et al. (2017) have proposed a phase diagram for bedforms in gravel-bed rivers, relating q* to the armour ratios (Figs. 16.5 and 16.9 in Venditti et al., 2017) that is comparable to our Fig. 10. Consequently, armour ratio varies in parallel to channel morphology, dominant macroforms (e.g. gravel bars, riffle-pool sequences), bed sediment mobility and streambed structures (e.g. clusters, stone cells) (as our review and meta-analysis showed). So, although it is a very simple indicator merely based on the grain size distribution, the armour ratio could be considered not only as some kind of metric of 'textural imprints' of sediment supply conditions, but also as a suitable proxy of the overall streambed organization and structuration in gravel-bed rivers (Venditti et al., 2017).

Finally, the limitations inherent to the data reanalysed in the present study should not be neglected. This data compilation was built after a careful review of the published literature on bedload transport (see references). We searched and selected for those case studies where there was access to bedload rating curves together with both surface and subsurface GSDs. To the best of our knowledge, there are not much more easily available data in the literature meeting these criteria. Consequently, the trends identified in this paper could be considered, in principle, based on an important amount of the bedload data generated by sediment transport research during the last decades. Nevertheless, the data have potential bias. First, there is variability within the compiled studies in how grain-size sampling was accomplished. This could be justified by the inherent difficulties of sampling grain size in highly heterogeneous and poorly sorted gravel-bed rivers, but one may pose the question about whether the data always represent a good estimate of the average streambed grain-size. Then, it can also be noticed that the data come mostly from mountain streams dominated by snowmelt flow regimes. Planning field-campaigns in order to measure bedload is easier in this kind of rivers compared to rainfall-dominated settings, where it is more difficult to know in advance when a channel-forming flow is going to occur. This explains the higher abundance of snowmelt-dominated streams in the dataset. Therefore, it is not easy to explore in depth the influence of other hydrological regimes based on the available data. Moreover, there is a strong geographical bias towards North America and USA, as outlined by other comparable review studies of gravel-bed river data (e.g. Phillips and Jerolmack, 2019). Field data are lacking from dryland, tropical regions, and/or cold environments. Consequently, there are some doubts as to whether some of the trends described here are globally representative of gravel-bed rivers. More field research would be welcomed to further explore the links between bedload supply and surface coarsening in natural gravel-bed rivers.

6. Concluding remarks

A large body of research in fluvial geomorphology has contributed to establishing the general idea that sediment supply, bedload fluxes, channel morphology, bankfull shear stresses, and surface grain size are intimately related in gravel-bed rivers. In this paper, we aimed to quantify the existing links between sediment supply and surface coarsening. Based on a meta-analysis of a large database of bedload discharge information for gravel-bed streams, we have proposed semi-empirical relations describing how surface grain-size and armour ratios evolve with the balance between bedload yield and channel sediment transport capacity. Armour ratios increase with decreasing bedload fluxes, as inferred from the dimensional analysis of bedload equations and as already shown by previous flume experiments.

Accounting for armouring is important for many reasons, since it influences the local availability of bedload, hydraulic roughness, bed permeability, and physical conditions for aquatic organisms. We believe that the empirical relationships found here between bedload yields and armour ratios have the potential to provide a quantitative framework for better exploring the links among surface armouring, hydraulics, and sediment availability in specific gravel-bed reaches and for developing more robust interpretations of textural adjustments to changes in sediment supply.

Notations

D	Grain-size (particle diameter)
D_{is}	*i*-th percentile of the surface grain-size distribution
D_{iss}	*i*-th percentile of the subsurface grain-size distribution
D_i^*	Armour ratio, or the ratio between the *i*-the percentiles of the surface and subsurface grain-size distributions
D_i^{**}	Corrected version of the armour ratio, i.e. armour ratio computed accounting for the inherent covariation between surface and subsurface grain sizes
f	Ratio between the armour ratio estimated based on the 84-th percentiles (D_{84}) and the armour ratio based on the median size (D_{50}) of the grain size distribution
GSD	Grain size distribution
ϕ	Bedload transport intensity (Einstein parameter)
q_s	Bedload transport rate per unit width
q_{ss}	Channel's bedload transport capacity (per unit width) to mobilize the subarmour sediment
q_{sss}	Channel's bedload transport capacity (per unit width) to mobilize the subarmour sediment
q^*	Bedload 'supply index', or the ratio between qss and qsss
Q	Peak discharge
Q_d	Peak discharge for the dominant discharge
Q/Q_d	Flow ratio
ω	Specific streampower
τ	Section-averaged bed shear stress
τ^*	Dimensionless (section-averaged) Shields shear stress
τ_c	Critical (section averaged) bed shear stress for sediment entrainment
τ_{cs}	Critical (section averaged) bed shear stress for the inception of motion of the surface sediment particles
τ_{css}	Critical (section averaged) bed shear stress for the inception of motion of the subsurface sediment particles
τ_{ci}^*	Critical threshold Shields stress for entrainment particle with sizes corresponding to the *i*-th percentile of the grain-size distribution

Uncited references

Andrews and Parker, 1987
Parker et al., 1982
Phillips et al., 2018
Powell et al., 2016

Declaration of Competing Interest

The authors declare that they have no known competing financial interests or personal relationships that could have appeared to influence the work reported in this paper.

Acknowledgements

The present work has been possible thanks to the financial support provided by the grant ACB17-44, co-funded by the post-doctoral 'Clarín' program-FICYT (Government of the Principality of Asturias) and the Marie Curie Co-Fund. This work was also performed within the framework of the EUR H2O'Lyon (ANR-17-EURE-0018) of Université de Lyon (UdL), within the program 'Investissements d'Avenir' operated by the French National Research Agency (ANR). We would like to thank Pablo Turrero García and Daniel Grace for their review of the English version of the manuscript.

Appendix A

Recking (2013b) proposed the following expression for bedload rates:

$$\phi = A \bullet \frac{\tau^{*\alpha}}{1 + \left(\frac{\tau_m^*}{\tau^*}\right)^{\beta}} \quad \text{Eq. S1}$$

where ϕ is the dimensionless transport rate, estimated using the Einstein parameter:

$$\phi = \frac{q_s}{\sqrt{g \bullet (s-1) \bullet D_{84}^3}} \quad \text{Eq. S2}$$

Coefficients A, α and β are three model parameters, for which values of 14, 2.5 and 4 were proposed, respectively (Recking, 2013b; Recking et al., 2016). τ_{m^*} is a mobility shear stress that allows to differentiate low transport conditions (with partial transport and bed clustering) apart from higher transport ones (Recking et al., 2016). Recking (2013b) estimates τ_{m^*} from:

$$\tau_m = (5 \bullet S + 0.06) \bullet \left(\frac{D_{84}}{D_{50}}\right)^{4.4 \bullet \sqrt{S} - 1.5} \quad \text{Eq. S3}$$

Eq. S3 is such that for low transport conditions ($\tau^* << \tau_m^*$):

$$\phi = A \bullet \frac{\tau^{*^{\alpha+\beta}}}{\tau_m^{\beta}} \quad \text{Eq. S4}$$

and for higher transport conditions ($\tau^* >> \tau_m^*$):

$$\phi = \tau^{*^{\alpha}} \quad \text{Eq. S5}$$

We can now combine equation S5 with the expression for the Einstein parameter (eq. S2):

$$q^* = \frac{q_{s_s}}{q_{s_{ss}}} = \frac{\phi_s}{\phi_{ss}} \bullet \left(\frac{D_{84ss}}{D_{84s}}\right)^{\frac{3}{2}} \quad \text{(S6)}$$

Incorporating now eq. S4 into eq. S6, we can deduce:

$$q^* = \left(\frac{\tau_s^*}{\tau_{ss}^*}\right)^{\alpha+\beta} \bullet \left(\frac{\tau_{m_s}^*}{\tau_{m_{ss}}^*}\right)^{\beta} \bullet \left(\frac{D_{84_s}}{D_{84_{ss}}}\right)^{\frac{3}{2}} \quad \text{Eq. S7}$$

for low transport conditions. Taking into account the expression for τ_m* (eq. S3) and assuming a similar bed slope for the surface and subsurface case:

$$\frac{\tau_{m_s}^*}{\tau_{m_{ss}}^*} = \left(\frac{D_{84_s}}{D_{84_{ss}}}\right) \bullet \left(\frac{D_{50_{ss}}}{D_{50_s}}\right) \quad \text{Eq. S8}$$

We could now introduce the idea that the armour ratio based on the D_{50} is linearly related to the value based on the D_{84} (see Fig. 3 in the main text of the paper):

$$\left(\frac{D_{84_s}}{D_{84_{ss}}}\right) = f \bullet \left(\frac{D_{50_s}}{D_{50_{ss}}}\right) \quad \text{Eq. S9}$$

Incorporating this idea into eq. S8, then:

$$\frac{\tau_{m_s}^*}{\tau_{m_{ss}}^*} = \frac{1}{f} \bullet \left(\frac{D_{84_s}}{D_{84_{ss}}}\right) \bullet \left(\frac{D_{84_s}}{D_{84_{ss}}}\right)^{-1} = \frac{1}{f} \quad \text{Eq. S10}$$

Now, we can simplify eq. S7 based on eq. S10:

$$q^* = \frac{1}{f} \bullet \left(\frac{\tau_s^*}{\tau_{ss}^*}\right)^{\alpha+\beta} \bullet \left(\frac{D_{84_s}}{D_{84_{ss}}}\right)^{\frac{3}{2}} \quad \text{Eq. S11}$$

Combining eq. S11 with that for the dimensionless Shields stress based on the D_{84}, then:

$$\begin{aligned} q^* &= \frac{1}{f} \bullet \left(\frac{D_{84_s}}{D_{84_{ss}}}\right)^{\frac{3}{2}-\alpha-\beta} \\ &= \frac{1}{f} \bullet \left(\frac{D_{84_s}}{D_{84_{ss}}}\right)^{-5} \\ &\rightarrow \left(\frac{D_{84_s}}{D_{84_{ss}}}\right) \\ &= f \bullet q^{*^{-\frac{1}{5}}} \end{aligned} \quad \text{Eq. S12}$$

at low transport conditions.

At high transport conditions (when $\tau^* >> \tau_m^*$), we should combine eq. S5 with eq. S6, and we arrive at:

$$q^* = \left(\frac{\tau_s^*}{\tau_{ss}^*}\right)^{\alpha} \bullet \left(\frac{D_{84_s}}{D_{84_{ss}}}\right)^{\frac{3}{2}} \quad \text{Eq. S13}$$

Combining this expression with that for the dimensionless Shields stress:

$$\begin{aligned} q^* &= \left(\frac{D_{84_s}}{D_{84_{ss}}}\right)^{\frac{3}{2}-\alpha} \\ &= \left(\frac{D_{84_s}}{D_{84_{ss}}}\right)^{-1} \\ &\rightarrow \left(\frac{D_{84_s}}{D_{84_{ss}}}\right) \\ &= q^{*^{-1}} \end{aligned} \quad \text{Eq. S14}$$

at full mobility conditions.

References

Allen, J.R.L., 1984. Sedimentary Structures, Their Character and Physical Basis. Elsevier, Amsterdam.

Almedeij, J.H., 2002. Bedload transport in gravel-bed streams under a wide range of Shields stresses. Ph.D. thesis Va. Polytech. Inst. and State Univ., Blacksburg.

Andrews, E.D., 1994. Marginal bed load transport in a gravel bed stream, Sagehen Creek. California. Water Resources Research 30, 2241–2250.

Andrews, E.D., Erman, D.C., 1986. Persistence in the size distribution of surficial bed material during an extreme snowmelt flood. Water Resour. Res. 22, 191–197.

Andrews, E.D., Parker, G., 1987. Formation of a coarse surface layer as the response to gravel mobility. In: Thorne, C.R., Bathurst, J.C., Hey, R.D. (Eds.), Sediment transport in gravel-bed rivers. Wiley, Chichester, pp. 269–300.

Bacchi, V., Recking, A., Eckert, N., Frey, P., Piton, G., Naaim, M., 2014. The effects of kinetic sorting on sediment mobility on steep slopes. Earth Surf. Process. Landf. 39, 1075–1086.

Bagnold, R.A., 1966. An approach to the sediment transport problem from general physics. In: U.S. Geol. Surv. Prof. Pap., 422-I.

Barry, J.J., Buffington, J.M., King, J.G., 2004. A general power equation for predicting bedload transport rates in gravel bed rivers. Water Resour. Res. 40, W104001.

Berni, C., Perret, E., Camenen, B., 2018. Characteristic time of sediment transport decrease in static armour formation. Geomorphology 317, 1–9.

Bertin, S., Friedrich, H., 2018. Effects of surface texture and structure on the development of stable fluvial armors. Geomorphology 306, 64–79.

Blom, A., Arkesteijn, L., Chavarrías, V., Viparelli, E., 2017. The equilibrium alluvial river under variable flow and its channel-forming discharge. Journal of Geophysical Research. Earth Surface 122, 1924–1948.

Borland, W.M., 1960. Stream Channel Stability. U.S. Bureau of Reclamation, Denver.

Brayshaw, A.C., 1984. Characteristics and origin of cluster bedforms in coarse-grained alluvial channels. Sedimentology of Gravels and Conglomerates 10, 77–85.

Brayshaw, A.C., Frostick, L.E., Reid, I., 1983. The hydrodynamics of particle clusters and sediment entrainment in coarse alluvial channels. Sedimentology 30, 137–143.

Buffington, J.M., 2012. Changes in channel morphology over human time scales. In: Church, M., Biron, P.M., Roy, A.G. (Eds.), Gravel-bed Rivers: Processes, Tools, Environments. 32, Wiley, Chichester, UK, pp. 435–463.

Buffington, J.M., Montgomery, D.R., 1999. A procedure for classifying textural facies in gravel-bed rivers. Water Resour. Res. 35 (6), 1903–1914.

Buffington, J.M., Montgomery, D.R., 1999. Effects of sediment supply on surface textures of gravel-bed rivers. Water Resour. Res. 35 (11), 3523–3530.

Buffington, J.M., Dietrich, W.E., Kirchner, J.W., 1992. Friction angle measurements on a naturally formed gravel streambed: implications for critical boundary shear stress. Water Resour. Res. 28 (2), 411–425.

Bunte, K., Abt, S.R., 2001. Sampling surface and subsurface particle-size distributions in wadable gravel-and cobble-bed streams for analyses in sediment transport, hydraulics, and streambed monitoring. In: Gen. Tech. Rep. RMRS-GTR-74. U.S. Department of Agriculture, Forest Service, Rocky Mountain Research Station, Fort Collins,CO, p. 428.

Butler, J.B., Lane, S.N., Chandler, J.H., 2001. Automated extraction of grain-size data for gravel surfaces using digital image processing. J. Hydraul. Res. 39, 519–529.

Camenen, B., Holubová, K., Lukac, M., Le Coz, J., Paquier, A., 2011. Assessment of Methods Used in 1D Models for Computing Bed-Load Transport in a Large River: The Danube River in Slovakia. J. Hydraul. Eng. 137 (10).

Carling, P.A., 1999. Subaqueous gravel dunes. J. Sediment. Res. 69, 534–545.

Carrillo, R., Mao, L., 2019. (2019). Relating coarse sediment transport dynamics with sediment sources in a glacier-fed Andean basin: Are sediments traceable from sources to sink?. Geophys. Res. Abstr. 21, EGU2019–15013.

Chin, A., Wohl, E., 2005. Toward a theory for step pool in stream channels. Prog. Phys. Geogr. 29, 275–296.

Chin, C.O., Melville, B.W., Raudkivi, A.J., 1994. Streambed armouring. J. Hydraul. Eng. 120 (8).

Church, M., 2006. Bed material transport and the morphology of alluvial river channels. Annu. Rev. Earth Planet. Sci. 34 (1), 325–354.

Church, M., Hassan, M.A., 2002. Mobility of bed material in Harris Creek. Water Resour. Res. 38 (11), 1237.

Church, M., Hassan, M., 2005. Upland gravel-bed rivers with low sediment transport. In: Garcia, C., Batalla, R.J. (Eds.), Catchment Dynamics and River Processes. Mediterranean and Other Climate Regions. Developments in Earth Surface Processes 7. Elsevier, Amsterdam, pp. 141–168.

Church, M., Rice, S.P., 2009. Form and growth of bars in a wandering gravel-bed river. Earth Surf. Process. Landf. 34, 1422–1432.
Church, M., Rood, K., 1983. Catalogue of alluvial river channel regime data. Dep. of Geography, Univ. of British Columbia, Vancouver.
Church, M., Zimmermann, A., 2007. Form and stability of step-pool channels: research progress. Water Resour. Res. 43, W03415.
Church, M.A., McLean, D.G., Wolcott, J.F., 1987. River Bed Gravels: Sampling and Analysis. In: Thorne, C.R., Bathurst, J.C., Hey, R.D. (Eds.), Sediments transport in Gravel Bed Rivers. John Wiley and Sons, New York, pp. 43–88.
Church, M., Hassan, M.A., Wolcott, J.F., 1998. Stabilizing self-organized structures in gravel-bed stream channels: Field and experimental observations. Water Resour. Res. 34 (11), 3169–3179.
Cin, R.D., 1968. Pebble clusters: their origin and utilization in the study of paleocurrents. Sediment. Geol. 2 (4), 233–241.
Clayton, J.A., Pitlick, J., 2008. Persistence of the surface texture of a gravel-bed river during a large flood. Earth Surf. Process. Landf. 33, 661–673.
Clifford, N.J., Richards, K.S., Robert, A., 1992. The influence of microform bed roughness elements on flow and sediment transport in gravel bed rivers: comment on a paper by Marwan A. Hassan and Ian Reid. Earth Surf. Process. Landf. 17, 529–534.
Cooper, J.R., Tait, S.J., 2009. Water-worked gravel beds in laboratory flumes – a natural analogue?. Earth Surf. Process. Landf. 34, 384–397.
Cui, Y., Parker, G., Lisle, T.E., Gott, J., Hansler-Ball, M.E., Pizzuto, J.E., Allmendinger, N.E., Reed, J.M., 2003. Sediment pulses in mountain rivers: 1. Experiments. Water Resour. Res. 39, 1239.
Curran, J., Waters, K.A., 2014. The importance of bed sediment sand content for the structure of a static armor layer in a gravel bed river. J. Geophys. Res. Earth Surf. 119, 1484–1497.
Dade, W.B., Renshaw, C.E., Magilligan, F.J., 2011. Sediment transport constraints on river response to regulation. Geomorphology 126 (1-2), 245–251.
Dietrich, W., Kirchner, J., Ikeda, H., Iseya, F., 1989. Sediment supply and the development of the coarse surface layer in gravel-bedded rivers. Nature 340, 215–217.
Eaton, B.C., Church, M.A., Millar, R.G., 2004. Rational regime model of alluvial channel morphology and response. Earth Surf. Process. Landf. 29 (4), 511–529.
Emmett, W.W., Seitz, H.R., 1974. Suspended- and bedload-sediment transport in the Snake and Clearwater rivers in the vicinity of Lewiston, Idaho (July 1973 through July 1974). U.S. Geological Survey, Boise, Idaho.
Erwin, S.O., Schmidt, J.C., Nelson, N.C., 2011. Downstream effects of impounding a natural lake: the Snake River downstream from Jackson Lake Dam, Wyoming. USA. Earth Surface Processes and Landforms 36, 1421–1434.
Ferdowsi, B., Ortiz, C.P., Houssais, M., Jerolmack, D.J., 2017. River-bed armouring as a granular segregation phenomenon. Nat. Commun. 8, 1363.
Ferguson, R.I., 2003. The missing dimension: effects of lateral variation on 1-D calculations of fluvial bedload transport. Geomorphology 56, 1–14.
Ferguson, R., 2007. Flow resistance equations for gravel and boulder bed streams. Water Resour. Res. 43 (W05427), 1–12.
Ferguson, R., Church, M., 2009. A critical perspective on 1-D modeling of river processes: gravel load and aggradation in lower Fraser River. Water Resour. Res. 45, W11424.
Ferrer-Boix, C., Hassan, M.A., 2014. Influence of the sediment supply texture on morphological adjustments in gravel-bed rivers. Water Resour. Res. 50, 8868–8890.
Ferrer-Boix, C., Hassan, M.A., 2015. Channel adjustments to a succession of water pulses in gravel bed rivers. Water Resour. Res. 51, 8773–8790.
Francalanci, S., Solari, L., Toffolon, M., Parker, G., 2012. Do alternate bars affect sediment transport and flow resistance in gravel-bed rivers?. Earth Surf. Process. Landf. 37 (8), 866–875.
Garde, R.J., Sahay, A., Bhatnagar, S., 2006. A simple mathematical model to predict the particle size distribution of the armour layer. J. Hydraul. Res. 44.
Gessler, J., 1967. The Beginning of Bedload Movement of Mixtures Investigated as Natural Armoring in Channels. In: W.M. Keck Laboratory of Hydraulics and Water Resources. California Institute of Technology, Pasadena, (Translation T-5).
Gessler, J., 1970. Self-stabilizing tendencies of alluvial channels. Journal of the Waterways, Harbors and Coastal Engineering Division, American Society of Civil Engineers 96 (2), 235–249.
Gintz, D., Hassan, M.A., Schmidt, K.H., 1996. Frequency and magnitude of bedload transport in a mountain river. Earth Surf. Process. Landf. 21, 433–445.
Gomez, B., 1983. Temporal variations in bedload transport rates: the effect of progressive bed armouring. Earth Surf. Process. Landf. 8 (1), 41–54.
Gomez, B., 1988. Two data sets describing channel-wide temporal variations in bedload-transport rates. 88-88, U.S. Geological Survey. Public Data File, 26.
Gomez, B., 1993. Roughness of stable, armored gravel beds. Water Resour. Res. 29 (11), 3631–3642.
Gomez, B., 1994. Effects of particle shape and mobility on stable armor development. Water Resour. Res. 30 (7), 2229–2239.
Harrison, H.S., 1950. Report on special investigations of bed sediment segregation in a degrading bed. Inst. of Eng. Res., University of California, Berkeley.
Haschenburger, J.K., 2017. Streambed Disturbance over a Long Flood Series. River Res. Appl. 33, 753–765.
Haschenburger, J.K., Wilcock, P.R., 2003. Partial transport in a natural gravel bed channel. Water Resour. Res. 39 (1), 1020.
Hassan, M.A., Church, M., 2000. Experiments on surface structure and partial sediment transport. Water Resour. Res. 36, 1885–1895.
Hassan, M.A., Church, M., 2001. Sensitivity of bed load transport in Harris Creek: Seasonal and spatial variation over a cobble-gravel bar. Water Resour. Res. 37 (3), 813–825.
Hassan, M.A., Reid, I., 1990. The influence of microform bed roughness elements on flow and sediment transport in gravel bed rivers. Earth Surf. Process. Landf. 15, 739–750.
Hassan, M.A., Zimmermann, A., 2012. Channel Response and Recovery to Changes in Sediment Supply. In: Church, M., Biron, P.M., Roy, A.G. (Eds.), Gravel-Bed Rivers: Processes, Tools, Environments. 33, Wiley & Sons, Chichester, UK, pp. 464–473.
Hassan, M.A., Egozi, R., Parker, G., 2006. Experiments on the effect of hydrograph characteristics on vertical grain sorting in gravel bed rivers. Water Resour. Res. 42, W09408.
Hassan, M.A., Smith, B.J., Hogan, D.L., Luzi, D.S., Zimmermann, A.E., Eaton, B.C., 2008. Sediment storage and transport in coarse bed streams: scale considerations. In: Rinaldi, M., Habersack, H., Piégay, H. (Eds.), Gravel-Bed Rivers VI: from process understanding to river restoration. Elsevier, Amsterdam, pp. 473–496.
Hassan, M.A., Saletti, M., Zhang, C., Ferrer-Boix, C., Johnson, J.P.L., Müller, T., von Flotow, C., 2020. Co-evolution of coarse grain structuring and bed roughness in response to episodic sediment supply in an experimental aggrading channel. Earth Surf. Process. Landf. 45, 948–961.
Haynes, H., Pender, G., 2007. Stress history effects on graded bed stability. J. Hydraul. Eng. 133 (4), 343–349.
Heays, K.G., Friedrich, H., Melville, B.W., 2014. Laboratory study of gravel-bed cluster formation and disintegration. Water Resour. Res. 50, 2227–2241.
Hinton, D., Hotchkiss, R.H., Cope, M., 2018. Comparison of Calibrated Empirical and Semi-Empirical Methods for Bedload Transport Rate Prediction in Gravel Bed Streams. J. Hydraul. Eng. 144 (7).
Hodge, R., Brasington, J., Richards, K., 2009. Analysing laser-scanned digital terrain models of gravel bed surfaces: linking morphology to sediment transport processes and hydraulics. Sedimentology 56, 2024–2043.
Jain, S., 1990. Armor or Pavement. Journal Hydraulic Engineering. ASCE 116, 436–440.
Jones, M.L., Seitz, H.R., 1980. Sediment transport in the Snake and Clearwater rivers in the vicinity of Lewiston, Idaho. U.S. Geological Survey. Open File Rep. 80-690, 179.
Kellerhals, R., Bray, D.L., 1971. Sampling procedures for coarse fluvial sediment. Journal of the Hydraulic Division. ASCE 97, 1165–1179.
King, J.G., Emmett, W.W., Whiting, P.J., Kenworthy, R.P., Barry, J.J., 2004. Sediment transport data and related information for selected gravel-bed streams and rivers in Idaho. In: U.S. For. Serv. Gen. Tech. Rep. RM, RMRS-GTR-131. p. 26.
Kirchner, J.W., Dietrich, W.E., Iseya, F., Ikeda, H., 1990. The variability of critical shear stress, friction angle, and grain protrusion in water-worked sediments. Sedimentology 37, 647–672.
Klaassen, G.J., 1988. Armoured river beds during flood. In: Tech. Rep. 394, Delft Hydraulics, Emmeloord, the Netherlands.
Klingeman, P. C. and Emmett, W. W. (1982). Gravel bedload transport processes. In: Hey, R.D., Bathurst, J. C. and Thorne, C. R. (eds.). *Gravel Bed Rivers: Fluvial Processes, Engineering and Management*, Wiley: Chichester; 141– 169.
Koster, E.H., 1978. Transverse ribs: their characteristics, origin, paleohydraulic significance. In: Miall, A.D. (Ed.), Fluvial Sedimentology, pp. 161-186. Canadian Society of Petroleum Geologists. Mem. p. 5.
Kuhnle, R.A., 1992. Fractional transport rates of bedload on Goodwin Creek. In: Billi, P. (Ed.), Dynamics of Gravel Bed Rivers. John Wiley, New York, pp. 141–155.
Kuhnle, R.A., Willis, J.C., 1992. Mean size distribution of bed load on Goodwin Creek. J. Hydraul. Eng. 118, 1443–1446.
Lamarre, H., Roy, A.G., 2008. A field experiment on the development of sedimentary structures in a gravel-bed river. Earth Surf. Process. Landf. 33, 1064–1081.
Lamarre, H., Roy, A.G., 2008. The role of morphology on the displacement of particles in a step–pool river system. Geomorphology 99, 270–279.
Lane, E.W., 1955. Design of stable channels. Transactions ASCE, Paper no. 2776 (20), 1234–1279.
Lane, E.W., 1955. The importance of fluvial geomorphology in hydraulic engineering. Proceedings of the American Society of Civil Engineers 81, (p. 745-741 - 745-717).
Laronne, J.B., Carson, M.A., 1976. Interrelationships between bed morphology and bed material transport for a small, gravel-bed channel. Sedimentology 23 (1), 67–85.
Laronne, J.B., Reid, I., 1993. Very high rates of bedload sediment transport by ephemeral desert rivers. Nature 366, 148–150.
Laronne, J.B., Reid, I., Yitshack, Y., Frostick, L.E., 1994. The non-layering of gravel streambeds under ephemeral flood regimes. J. Hydrol. 159 (1-4), 353–363.
Lawson, D., 2020. Towards bed state morphodynamics in gravel-bed rivers. Prog. Phys. Geogr. 1–27.
Lenzi, M.A., D'Agostino, V., Billi, P., 1999. Bedload transport in the instrumented catchment of the Rio Cordon. Part I: analysis of bedload records, conditions and threshold of bedload entrainment. Catena 36, 171–190.
Lenzi, M., Mao, L., Comiti, F., 2004. Magnitude-frequency analysis of bed load data in an Alpine boulder bed stream. Water Resour. Res. 40.
Lindeman, R.H., Merenda, P.F., Gold, R.Z., 1980. Introduction to Bivariate and Multivariate Analysis. Glenview, IL, USA, Scott Foresman & Co.
Lisle, T.E., 1986. Stabilization of a gravel channel by large streamside obstruction and bedrock bends, Jacoby Creek, northwestern California. Geol. Soc. Am. Bull. 97, 999–1011.
Lisle, T.E., 1989. Sediment transport and resulting deposition in spawning gravels, north coastal California. Water Resour. Res. 25, 1303–1319.
Lisle, T.E., 1995. Particle size variations between bed load and bed material in natural gravel bed channels. Water Resour. Res. 31, 1107–1118.
Lisle, T.E., Hilton, T., 1992. The volume of fine sediment in pools: an index of sediment supply in gravel-bed streams. Water Resour. Bull. 28 (2), 371–383.
Lisle, T.E., Madej, M.A., 1992. Spatial variation in armouring in a channel with high sediment supply. In: Billi, P., Hey, R.D., Thorne, C.R., Tacconi, P. (Eds.), Dynamics of Gravel-bed Rivers. John Wiley and Sons, pp. 277–293.
Little, W.C., Mayer, P.G., 1972. The role of sediment gradation of channel armoring. In: Publ. ERC-0672, 104 pp., Ga. Inst. of Technol.
Madej, M.A., Ozaki, V., 1996. Channel response to sediment wave propagation and movement, Redwood Creek, California. USA. Earth Surface Processes and Landforms 21, 911–927.
Mao, L., 2012. The effect of hydrographs on bed load transport and bed sediment spatial arrangement. J. Geophys. Res. Earth Surf. 117 (F3).
Mao, L., 2018. The effects of flood history on sediment transport in gravel-bed rivers. Geomorphology 322, 196–205.
Mao, L., Cooper, J.R., Frostick, L.E., 2011. Grain size and topographical differences between static and mobile armour layers. Earth Surf. Process. Landf. 36, 1321–1334.

Marion, A., Fraccarollo, L., 1997. Experimental investigation of mobile armoring development. Water Resour. Res. 33, 1447–1453.

Marion, A., Tait, S.J., McEwan, I.K., 2003. Analysis of small-scale gravel bed topography during armoring. Water Resour. Res. 39 (12).

Masteller, C.C., Finnegan, N.J., Turowski, J.M., Yager, E.M., Rickenmann, D., 2019. History-dependent threshold for motion revealed by continuous bedload transport measurements in a steep mountain stream. Geophys. Res. Lett. 46, 2583–2591.

McLean, D.G., Church, M., Tassone, B., 1999. Sediment transport along lower Fraser River: 1. Measurements and hydraulic computations. Water Resour. Res. 35, 2533–2548.

Métivier, F., Barrier, L., 2012. Alluvial landscape evolution: what do we know about metamorphosis of gravel bed meandering and braided streams?. In: Church, M., Biron, P., Roy, A. (Eds.), Gravel-bed Rivers: processes, tools, environments, chapter. 34, Wiley & Sons, Chichester, pp. 474–501.

Métivier, F., Lajeunesse, E., Devauchelle, O., 2017. Laboratory rivers: Lacey's law, threshold theory, and channel stability. Earth Surface Dynamics 5, 187–198.

Milhous, R.T., 1973. Sediment transport in a gravel-bottomed stream. Ph.D. thesis Oregon State University, Corvallis.

Misset, C., Recking, A., Legout, C., Bakker, M., Bodereau, N., Borgniet, L., Cassel, M., Geay, T., Gimbert, F., Navratil, O., Piegay, H., Valsangkar, N., Cazilhac, M., Poirel, A., Zanker, S., 2020. Combining multi-physical measurements to quantify bedload transport and morphodynamic interactions in an alpine braiding river reach. Geomorphology

Monteith, H., Pender, G., 2005. Flume investigations into the influence of shear stress history on a graded sediment bed. Water Resour. Res. 41, W12401.

Montgomery, D.R., Buffington, J.M., 1997. Channel-reach morphology in mountain drainage basins. Geol. Soc. Am. Bull. 109, 596–611.

Moog, D.B., Whiting, P.J., 1998. Annual hysteresis in bed load rating curves. Water Resour. Res. 34 (9), 2393–2399.

Mueller, E.R., Pitlick, J., 2005. Morphologically based model of bed load transport capacity in a headwater stream. J. Geophys. Res. 110, F02016.

Mueller, E.R., Pitlick, J., 2014. Sediment supply and channel morphology in mountain river systems: 2. Single thread to braided transitions. J. Geophys. Res. Earth Surf. 119, 1516–1541.

Mueller, E.R., Pitlick, J., Nelson, J.M., 2005. Variation in the reference Shields stress for bed load transport in gravel-bed streams and rivers. Water Resour. Res. 41, W04006.

Muskatirovic, J., 2008. Analysis of bedload transport characteristics of Idaho streams and rivers. Earth Surf. Process. Landf. 33, 1757–1768.

Nelson, P.A., Venditti, J.G., Dietrich, W.E., Kirchner, J.W., Ikeda, H., Iseya, F., Sklar, L.S., 2009. Response of bed surface patchiness to reductions in sediment supply. J. Geophys. Res. 114, F02005.

Nelson, P.A., Dietrich, W.E., Venditti, J.G., 2010. Bed topography and the development of forced bed surface patches. J. Geophys. Res. 115.

Nikora, V.I., Goring, D.G., Biggs, B.J.F., 1998. On gravel bed roughness characterization. Water Resour. Res. 34 (3), 517–527.

Ockelford, A., Haynes, H., 2013. The impact of stress history on bed structure. Earth Surf. Process. Landf. 38 (7), 717–727.

Ockelford, A., Woodcock, S., Haynes, H., 2019. The impact of inter-flood duration on non-cohesive sediment bed stability. Earth Surf. Process. Landf. 44, 2861–2871.

Odgaard, J., 1984. Flow and Bed Topography in Alluvial Channel Bend. J. Hydraul. Eng. 110 (4).

Oldmeadow, D.F., Church, M., 2006. A field experiment on streambed stabilization by gravel structures. Geomorphology 78, 335–350.

Orrú, C., Blom, A., Uijttewaal, W.S.J., 2016. Armor breakup and reformation in a degradational laboratory experiment. Earth Surface Dynamics 4, 461–470.

Paola, C., 1989. Topographic sorting. Eos. Transactions. 70, American Geophysical Union, 332.

Paphitis, D., Collins, M.B., 2005. Sand grain threshold, in relation to bed Stress history: an experimental study. Sedimentology 52, 827–838.

Parker, G., 1978. Self-formed rivers with equilibrium banks and mobile bed: Part II. The gravel river. J. Fluid Mech. 89 (1), 127–148.

Parker, G., 1979. Hydraulic geometry of active gravel rivers. Journal of the Hydraulics Division. American Society of Civil Engineers 105 (HY9), 1185–1201.

Parker, G., 1990. Surface-based bedload transport relation for gravel rivers. J. Hydraul. Res. 28, 417–436.

Parker, G., 2004. 1D Sediment Transport Morphodynamics with Applications to Rivers and Turbidity Currents. In: Copyrighted ebook, available at: http://hydrolab.illinois.edu/people/parkerg//morphodynamics_e-book.htm.

Parker, G., 2008. Transport of Gravel and Sediment Mixtures. In: García, M. (Ed.), Sedimentation Engineering: Processes, Measurements, Modeling, and Practice. Manual and Reports in Engineering Practice No. 110 American Society of Civil Engineers, Reston, VA, pp. 165–264.

Parker, G., Klingeman, P.C., 1982. On why gravel bed streams are paved. Water Resour. Res. 18 (5), 1409–1423.

Parker, G., Sutherland, A.J., 1990. Fluvial armor. J. Hydraul. Res. 28 (5), 529–544.

Parker, G., Toro-Escobar, C.M., 2002. Equal mobility of gravel in streams: The remains of the day. Water Resour. Res. 38 (11), 1264.

Parker, G., Klingeman, P.C., McLean, D.C., 1982. Bedload and size distribution in paved, gravel-bed streams. Proceedings of the American Society of Civil Engineers, Journal of the Hydraulics Division 108, 544–571.

Parker, G., Wilcock, P.R., Paola, C., Dietrich, W.E., Pitlick, J., 2007. Physical basis for quasi-universal relations describing bankfull hydraulic geometry of single-thread gravel bed rivers. J. Geophys. Res. 112, F04005.

Perret, E., Berni, C., Camenen, B., 2020. How does the bed surface impact low-magnitude bedload transport rates over gravel-bed rivers?. Earth Surf. Process. Landf.

Pfeiffer, A.M., Finnegan, N.J., 2018. Regional variation in gravel riverbed mobility, controlled by hydrologic regime and sediment supply. Geophys. Res. Lett. 45, 3097–3106.

Pfeiffer, A.M., Finnegan, N.J., Willenbring, J.K., 2017. Sediment supply controls gravel river geometry. Proc. Natl. Acad. Sci. 114 (13), 3346–3351.

Phillips, C.B., Jerolmack, D.J., 2016. Self-organization of river channels as a critical filter on climate signals. Science 352 (6286), 694–697.

Phillips, C.B., Jerolmack, D.J., 2019. Bankfull transport capacity and the threshold of motion in coarse-grained rivers. Water Resour. Res. 55, 11316–11330.

Phillips, C.B., Hill, K.M., Paola, C., Singer, M.B., Jerolmack, D.J., 2018. Effect of flood hydrograph duration, magnitude, and shape on bed load transport dynamics. Geophys. Res. Lett. 45, 8264–8271.

Piedra, M.M., Haynes, H., Hoey, T.B., 2012. The spatial distribution of coarse surface grains and the stability of gravel river beds. Sedimentology 59, 1014–1029.

Pitlick, J., Mueller, E.R., Segura, C., Cress, R., Torizzo, M., 2008. Relation between flow, surface layer armoring and sediment transport in gravel bed rivers. Earth Surf. Process. Landf. 33, 1192–1209.

Pitlick, J., Mueller, E.R., Segura, C., 2012. Differences in sediment supply to braided and single-thread channels: what do the data tell us?. In: Church, M., Biron, P.M., Roy, A.G. (Eds.), Gravel-Bed Rivers: Processes, Tools, Environments, chapter. 35, Wiley & sons, Chichester, U. K, pp. 502–511.

Piton, G., Recking, A., 2017. The concept of travelling bedload and its consequences for bedload computation in mountain streams. Earth Surf. Process. Landf. 42, 1505–1519.

Plumb, B.D., Juez, C., Annable, W.K., McKie, C.W., Franca, M.J., 2019. The impact of hydrograph variability and frequency on sediment transport dynamics in a gravel-bed flume. Earth Surf. Process. Landf. 2019.

Powell, D.M., Reid, I., Laronne, J.B., 2001. Evolution of bed load grain size distribution with increasing flow strength and the effect of flow duration on the caliber of bed load sediment yield in ephemeral gravel bed rivers. Water Resour. Res. 37 (5), 1463–1474.

Powell, D.M., Ockelford, A., Rice, S.P., Hillier, J.K., Nguyen, T., Reid, I., Tate, N.J., Ackerley, D., 2016. Structural properties of mobile armors formed at different flow strengths in gravel-bed rivers. J. Geophys. Res. Earth Surf. 121, 1494–1515.

Proffitt, G.T., Sutherland, A.J., 1983. Transport of non uniform sediments. J. Hydraul. Res. 21 (1), 33–43.

Recking, A., 2010. A comparison between flume and field bed load transport data and consequences for surface based bed load transport prediction. Water Resour. Res. 46, W03518.

Recking, A., 2012. Influence of sediment supply on mountain streams bedload transport. Geomorphology 175-176, 139–150.

Recking, A., 2013. An analysis of nonlinearity effects on bed load transport prediction. J. Geophys. Res. Earth Surf. 118, 1264–1281.

Recking, A., 2013. Simple method for calculating reach-averaged bed-load transport. J. Hydraul. Eng. 139 (1), 70–75.

Recking, A., Bacchi, V., Naaim, M., Frey, P., 2009. Antidunes on steep slopes. J. Geophys. Res. 114, F04025.

Recking, A., Leduc, P., Liébault, F., Church, M., 2012. A field investigation of the influence of sediment supply on step-pool morphology and stability. Geomorphology 139–140, 53–66.

Recking, A., Piton, G., Vázquez-Tarrío, D., Parker, G., 2016. Quantifying the morphological print of bedload transport. Earth Surf. Process. Landf. 41 (6), 809–822.

Reid, I., Frostick, L.E., 1984. Particle interaction and its effect on the thresholds of initial and final bedload motion in coarse alluvial channels. In: Koster, E.H., Steel, R.J. (Eds.), Sedimentology of Gravels and Conglomerates. 10, Canadian Society of Petroleum Geologists, Memoir, pp. 61–68.

Reid, I., Frostick, L.E., 1986. Dynamics of bedload transport in Turkey Brook, a coarse-grained alluvial channel. Earth Surf. Process. Landf. 11, 143–155.

Reid, I., Hassan, M.A., 1992. The influence of microform bed roughness elements on flow and sediment transport in gravel bed rivers: A reply. Earth Surf. Process. Landf. 17, 535–538.

Reid, I., Laronne, J.B., 1995. Bedload sediment transport in an ephemeral stream and a comparison with seasonal and perennial counterparts. Water Resour. Res. 31, 773–781.

Reid, I., Frostick, L.E., Layman, J.T., 1985. The incidence and nature of bed load transport during flows in coarse-grained alluvial channels. Earth Surf. Process. Landf. 10, 33–44.

Reid, I., Frostick, L.E., Brayshaw, A.C., 1992. Microform roughness elements and the selective entrainment and entrapment of particles in gravel-bed rivers. In: Billi, P., Hey, R.D., Thorne, C.R., Tacconi, P. (Eds.), Dynamics of Gravel bed Rivers. Wiley, Chichester, pp. 253–266.

Reid, I., Laronne, J.B., Powell, D.M., 1995. The Nahal Yatir bedload database: Sediment dynamics in a gravel-bed ephemeral stream. Earth Surf. Process. Landf. 20, 845–857.

Rice, S.P., Haschenburger, J.K., 2004. A hybrid method for size characterization of coarse subsurface fluvial sediments. Earth Surf. Process. Landf. 29, 373–389.

Richards, K., Clifford, N., 1991. Fluvial geomorphology: structured beds in gravelly rivers. Prog. Phys. Geogr. 15 (4), 407–411.

Rickenmann, D., Recking, A., 2011. Evaluation of flow resistance in gravel-bed rivers through a large field data set. Water Resour. Res. 47, W07538.

Rollet, A.J., Piégay, H., Dufour, S., Bornette, G., Persat, H., 2014. Assessment of consequences of sediment deficit on a gravel river bed downstream of dams in restoration perspectives: application of a multicriteria. hierarchical and spatially explicit diagnosis. River Research and Applications 30, 939–953.

Ryan, S.E., Emmett, W.W., 2002. The nature of flow and sediment movement in Little Granite Creek near Bondurant, Wyoming. In: Gen. Tech. Rep. RMRS-GTR-90. Ogden, UT. U.S. Department of Agriculture, Forest Service, Rocky Mountain Research Station, p. 48.

Ryan, S.E., Porth, L.S., Troendle, C.A., 2002. Defining phases of bedload transport using piecewise regression. Earth Surf. Process. Landf. 27, 971–990.

Ryan, S.E., Porth, L.S., Troendle, C.A., 2005. Coarse sediment transport in mountain streams in Colorado and Wyoming, USA. Earth Surf. Process. Landf. 30, 269–288.

Schmidt, J.C., Wilcock, P.R., 2008. Metrics for assessing the downstream effects of dams. Water Resour. Res. 44, W04404.

Seitz, H.R., 1977. Suspended- and bedload- sediment transport in the Snake and Clearwater rivers in the vicinity of Lewiston, Idaho (August 1975 through July 1976). Boise, Idaho, U.S. Geological Survey. Open File Rep. 76-886, 77.
Sklar, L.S., Fadde, J., Venditti, J.G., Nelson, P., Wydzga, M.A., Cui, Y., Dietrich, W.E., 2009. Translation and dispersion of sediment pulses in flume experiments simulating gravel augmentation below dams. Water Resour. Res. 45, W08439.
Smart, G., Aberle, J., Duncan, M., Walsh, J., 2004. Measurement and analysis of alluvial bed roughness. J. Hydraul. Res. 42 (3).
Turowski, J., Yager, E.M., Badoux, A., Rickenmann, D., Molnar, P., 2009. The impact of exceptional events on erosion, bedload transport and channel stability in a step-pool cannel. Earth Surf. Process. Landf. 34 (12), 1661–1673.
Turowski, J.M., Badoux, A., Rickenmann, D., 2011. Start and end of bedload transport in gravel-bed streams. Geophys. Res. Lett. 38, L04401.
Vázquez-Tarrío, D., Batalla, R.J., 2019. Assessing controls on the displacement of tracers in gravel-bed rivers. Water 11 (8), 1598.
Vázquez-Tarrío, D., Fernández-Iglesias, E., Fernández García, M., Marquínez, J., 2019. Quantifying the Variability in flow competence and streambed mobility with water discharge in a gravel-bed channel: River Esva, NW Spain. Water 11, 2662.
Vázquez-Tarrío, D., Recking, A., Liébault, F., Tal, M., Menéndez-Duarte, R., 2019. Particle transport in gravel-bed rivers: Revisiting passive tracer data. Earth Surf. Process. Landf. 44, 112–128.
Vázquez-Tarrío, D., Tal, M., Camenen, B., Piégay, H., 2019. Effects of continuous embankments and successive run-of-the-river dams on bedload transport capacities along the Rhône River, France. Sci. Total Environ. 658, 1375–1389.
Venditti, J.G., Dietrich, W.E., Nelson, P.A., Wydzga, M.A., Fadde, J., Sklar, L.S., 2005. Can coarse surface layers in gravel-bedded rivers be mobilized by finer gravel bedload?. Eos Trans. AGU 86 (52), (Fall Meet. Suppl., Abstract H51H-05).
Venditti, J.G., Dietrich, W.E., Nelson, P.A., Wydzga, M.A., Fadde, J., Sklar, L.S., 2010. Mobilization of coarse surface layers in gravel-bedded rivers by finer gravel bed load. Water Resour. Res. 46, W07506.
Venditti, J.G., Dietrich, W.E., Nelson, P.A., Wydzga, M.A., Fadde, J., Sklar, L.S., 2010. Effect of sediment pulse grain size on sediment transport rates and bed mobility in gravel bed rivers. J. Geophys. Res. Earth Surf. 115, F03039.
Venditti, J.G., Nelson, P.A., Bradley, R.W., Haught, D., Gitto, A.B., 2017. Bedforms, structures, patches, and sediment supply in gravel-bed rivers. In: Tsutsumi, D., Laronne, J.B. (Eds.), Gravel-Bed Rivers: Processes and Disasters, chapter 16, 439– 466. Wiley & Sons, Chichester, UK.
Vericat, D., Batalla, R.J., Garcia, C., 2006. Breakup and reestablishment of the armour layer in a large gravel-bed river below dams: the lower Ebro. Geomorphology 76, 122–136.
Wang, T., Liu, X., 2009. The Breakup of Armor Layer in a Gravel Bed Stream with No Sediment Supply. In: Zhang, C., Tang, H. (Eds.), Advances in Water Resources and Hydraulic Engineering, Proceedings of 16th IAHR-APD Congress and 3rd Symposium of IAHR-ISHS. Springer Berlin Heidelberg, pp. 919–923.
Warburton, J., 2007. Mountain Environments. In: Perry, C., Taylor, K. (Eds.), Environmental Sedimentology. Blackwell, Oxford.
Wathen, S.J., Ferguson, R.I., Hoey, T.B., Werritty, A., 1995. Unequal mobility of sand and gravel in weakly bimodal sediment. Water Resour. Res. 31, 2087–2096.
Whiting, P.J., Dietrich, W.E., Leopold, L.B., Drake, T.G., Shreve, R.L., 1988. Bedload sheets in heterogeneous sediment. Geology 16, 105–108.
Wilcock, P.R., 2001. The flow, the bed, and the transport: interaction in flume and field. In: Mosley, P. (Ed.), Proceedings of the Fifth Gravel-Bed Rivers Workshop. New Zealand Hydrological Society, Wellington, pp. 183–219.
Wilcock, P.R., DeTemple, B.T., 2005. Persistence of armor layers in gravel-bed streams. Geophys. Res. Lett. 32, L08402.
Wilcock, P.R., Kenworthy, S.T., 2002. A two-fraction model for the transport of sand/gravel mixtures. Water Resour. Res. 38 (10), 1194.
Wilcock, P.R., McArdell, B.W., 1993. Surface-based fractional transport rates: Mobilization thresholds and partial transport of a sand-gravel sediment. Water Resour. Res. 29, 1297–1312.
Wilcock, P.R., McArdell, B.W., 1997. Partial transport of a sand/gravel sediment. Water Resour. Res. 33, 235–245.
Wilcock, P., Pitlick, J., Cui, Y., 2009. Sediment transport primer: estimating bed-material transport in gravel-bed rivers. In: Gen. Tech. Rep. RMRS-GTR-226. Fort Collins, CO: U.S. Department of Agriculture, Forest Service, Rocky Mountain Research Station, p. 78.
Willets, B.B., Maizels, J.K., Florence, J., 1988. The simulation of streambed armouring and its consequences. Proc. Inst. Civ. Eng. 84 (3), 615–617.
Williams, G.P., Rosgen, D.L., 1989. Measured total sediment loads (suspended loads and bedloads) for 93 United States streams. U.S. Geological Survey. Open File Report 89-67, 128.
Wittenberg, L., Newson, M.D., 2005. Particle clusters in gravel-bed rivers: an experimental morphological approach to bed material transport and stability concepts. Earth Surf. Process. Landf. 30, 1351–1368.
Wittenberg, L., Laronne, J.B., Newson, M.D., 2007. Bed clusters in humid perennial and Mediterranean ephemeral gravel-bed streams: The effect of clast size and bed material sorting. J. Hydrol. 334 (3-4), 312–318.
Wolman, M., 1954. A method for sampling coarse river-bed material. American Geophysical Union Transactions 35 (951–956), 1954.
Yager, E., Kenworthy, M., Monsalve, A., 2015. Taking the river inside: Fundamental advances from laboratory experiments in measuring and understanding bedload transport processes. Geomorphology 244, 21–32.
Yager, E.M., Venditti, J.G., Smith, H., Schmeeckle, M., 2018. The trouble with shear stress. Geomorphology 323, 41–50.
Yalin, M.S., 1972. Mechanics of Sediment Transport. Pergamon Press.
Zimmermann, A., Church, M., 2001. Channel morphology, gradient profiles and bed stresses during flood in a step-pool channel. Geomorphology 40, 311–332.